



On the efficacy of a control volume finite element method for the capture of patterns for a volume-filling chemotaxis model

Moustafa Ibrahim, Mazen Saad

► To cite this version:

Moustafa Ibrahim, Mazen Saad. On the efficacy of a control volume finite element method for the capture of patterns for a volume-filling chemotaxis model. Computers and Mathematics with Applications, Elsevier, 2014, <http://www.sciencedirect.com/science/article/pii/S0898122114001333>. <10.1016/j.camwa.2014.03.010>. <hal-01131413>

HAL Id: hal-01131413

<https://hal.archives-ouvertes.fr/hal-01131413>

Submitted on 13 Mar 2015

HAL is a multi-disciplinary open access archive for the deposit and dissemination of scientific research documents, whether they are published or not. The documents may come from teaching and research institutions in France or abroad, or from public or private research centers.

L'archive ouverte pluridisciplinaire **HAL**, est destinée au dépôt et à la diffusion de documents scientifiques de niveau recherche, publiés ou non, émanant des établissements d'enseignement et de recherche français ou étrangers, des laboratoires publics ou privés.

On the efficacy of a control volume finite element method for the capture of patterns for a volume-filling chemotaxis model

Moustafa Ibrahim, Mazen Saad

*École Centrale de Nantes.
Département Informatique et Mathématiques.
Laboratoire de Mathématiques Jean Leray (UMR 6629 CNRS).
1, rue de la Noë, BP 92101, F-44321 Nantes, France*

Abstract

In this paper, a *control volume finite element scheme* for the capture of spatial patterns for a volume-filling chemotaxis model is proposed and analyzed. The diffusion term, which generally involves an anisotropic and heterogeneous diffusion tensor, is discretized by piecewise linear conforming triangular finite elements (P1-FEM). The other terms are discretized by means of an upstream finite volume scheme on a dual mesh, where the dual volumes are constructed around the vertices of each element of the original mesh. The scheme ensures the validity of the discrete maximum principle under the assumption that the transmissibility coefficients are nonnegative. The convergence analysis is based on the establishment of a priori estimates on the cell density, these estimates lead to some compactness arguments in L^2 based on the use of the Kolmogorov compactness theorem. Finally, we show some numerical results to illustrate the effectiveness of the scheme to capture the pattern formation for the mathematical model.

Keywords: Finite volume scheme, Finite element method, Volume-filling, Chemotaxis, Heterogeneous anisotropic tensor, Patterns.

1. Introduction

Patterns are the solutions of a reaction-diffusion system which are stable in time and stationary inhomogeneous in space, while pattern formation in mathematics refers to the process that, by changing a bifurcation parameter, the spatially homogeneous steady states lose stability to spatially inhomogeneous perturbations, and stable inhomogeneous solutions arise.

The pattern formation has been successfully applied to bacteria (see e.g. [1]) where we investigate specific and necessary parameters to obtain stationary distribution of the disease. Also, it has been applied to skin pigmentation patterns [2] to understand the diversity of patterns on the animal coat pattern, and many other examples.

The pattern formation depends on two key properties: the first is to apply the seminal idea of Turing [3] for a reaction-diffusion system and consequently determine the bifurcation parameters for the generation of stationary inhomogeneous spatial patterns (also called Turing Patterns), and the second is to apply a robust scheme to numerically investigate and capture the generation of spatio-temporal patterns. One of the most popular reaction-diffusion systems that can generate spatial patterns is the chemotaxis model.

Email addresses: `moustafa.ibrahim@ec-nantes.fr` (Moustafa Ibrahim), `mazen.saad@ec-nantes.fr` (Mazen Saad)

Chemotaxis is the feature movement of a cell along a chemical concentration gradient either towards the chemical stimulus, and in this case the chemical is called chemoattractant, or away from the chemical stimulus and then the chemical is called chemorepellent. The mathematical analysis of chemotaxis models shows a plenitude of spatial patterns such as the chemotaxis models applied to skin pigmentation patterns [4, 5] that lead to aggregations of one type of pigment cell into a striped spatial pattern. Other models have been successfully applied to the aggregation patterns in an epidemic disease [6], tumor growth [7], angiogenesis in tumor progression [8], and many other examples. Theoretical and mathematical modeling of chemotaxis dates to the pioneering works of Patlak in the 1950s [9] and Keller and Segel in the 1970s [10, 11]. The review article by Horstmann [12] provides a detailed introduction into the mathematics of the Keller-Segel model for chemotaxis.

In this paper, we present and study a numerical scheme for the capture of spatial patterns for a nonlinear degenerate volume-filling chemotaxis model over a general mesh, and with inhomogeneous and anisotropic diffusion tensors. Recently, the convergence analysis of a finite volume scheme for a degenerate chemotaxis model over a homogeneous domain has been studied by Andreianov *et al.* [13], where the diffusion tensor is considered to be proportional to the identity matrix, and the mesh used for the space discretization is assumed to be admissible in the sense of satisfying the orthogonality condition as in [14]. The upwind finite volume method used for the discretization of the convective term ensures stability and is extremely robust and computationally inexpensive. However, standard finite volume scheme does not permit handling anisotropic diffusion on general meshes, even if the orthogonality condition is satisfied. The reason for this is that there is no straightforward way to apply the finite volume scheme to problems with full diffusion tensors. Various “multi-point” schemes, where the approximation of the flux through an edge involves several scalar unknowns, have been proposed, see for e.g. [15, 16] for the so-called SUCHI scheme, [17, 18] for the so-called gradient scheme, and [19] for the development of the so-called DDFV schemes.

To handle the discretization of the anisotropic diffusion, it is well-known that the finite element method allows for an easy discretization of the diffusion term with a full tensor. However, it is well-established that numerical instabilities may arise in the convection-dominated case. To avoid these instabilities, the theoretical analysis of the *control volume finite element method* has been carried out for the case of degenerate parabolic problems with full diffusion tensors. Schemes with mixed conforming piecewise linear finite elements on triangles for the diffusion term and finite volumes on dual elements were proposed and studied in [20, 21, 22, 23, 24] for fluid mechanics equations, are indeed quite efficient.

Afif and Amaziane analyzed in [23] the convergence of a vertex-centered finite volume scheme for a nonlinear and degenerate convection-diffusion equation modeling a flow in porous media and without reaction term. This scheme consists of a discretization of the Laplacian by the piecewise linear conforming finite element method (see also [25, 26]), the effectiveness of this scheme was tested in benchmarks of FVCA series of conferences [27]. Cariaga *et al.* in [24] considered the same scheme for a reaction-diffusion-convection system, where the velocity of the fluid flow is considered to be constant in the convective term.

The intention of this paper is to extend the ideas of [13, 23, 24] to a fully nonlinear degenerate parabolic systems modeling the effect of volume-filling for chemotaxis. In order to discretize this class of systems, we discretize the diffusion term by means of piecewise linear conforming finite element. The other terms are discretized by means of a finite volume scheme on a dual mesh (Donald mesh), with an upwind discretization of the numerical flux of the convective term to ensure the stability and the maximum principle of the scheme, where the dual mesh is constructed

around the vertex of every triangle of the primary mesh.

The rest of this paper is organized as follows. In Section 2, we introduce the chemotaxis model based on realistic biological assumptions, which incorporates the effect of volume-filling mechanism and leads to a nonlinear degenerate parabolic system. In Section 3, we derive the *control volume finite element scheme*, where an upwind finite volume scheme is used for the approximation of the convective term, and a standard P1-finite element method is used for the diffusive term. In Section 4, by assuming that the transmissibility coefficients are nonnegative, we prove the maximum principle and give the *a priori* estimates on the discrete solutions. In Section 5, we show the compactness of the set of discrete solutions by deriving estimates on difference of time and space translates for the approximate solutions. Next, in Section 6, using the Kolmogorov relative compactness theorem, we prove the convergence of a sequence of the approximate solutions, and we identify the limits of the discrete solutions as weak solutions of the parabolic system proposed in Section 2. In the last section, we present some numerical simulations to capture the generation of spatial patterns for the volume-filling chemotaxis model with different tensors. These numerical simulations are obtained with our *control volume finite element scheme*.

2. Volume-filling chemotaxis model

We are interested in the *control volume finite element scheme* for a nonlinear, degenerate parabolic system formed by convection-diffusion-reaction equations. This system is complemented with homogeneous zero flux boundary conditions, which correspond to the physical behavior of the cells and the chemoattractant. The modified Keller-Segel system that we consider here, is very similar to that of Andreianov *et al.* [13], to which we have added tensors for the diffusion terms. Specifically, we consider the following system:

$$\begin{cases} \partial_t u - \operatorname{div} (\Lambda(x) a(u) \nabla u - \Lambda(x) \chi(u) \nabla v) = f(u) & \text{in } Q_T, \\ \partial_t v - \operatorname{div} (D(x) \nabla v) = g(u, v) & \text{in } Q_T, \end{cases} \quad (2.1)$$

with the boundary conditions on $\Sigma_T := \partial\Omega \times (0, T)$ given by

$$(\Lambda(x) a(u) \nabla u - \Lambda(x) \chi(u) \nabla v) \cdot \eta = 0, \quad D(x) \nabla v \cdot \eta = 0, \quad (2.2)$$

and the initial conditions given by:

$$u(x, 0) = u_0(x), \quad v(x, 0) = v_0(x), \quad x \in \Omega. \quad (2.3)$$

Herein, $Q_T := \Omega \times (0, T)$, $T > 0$ is a fixed time, and Ω is an open bounded polygonal domain in \mathbb{R}^2 , with Lipschitz boundary $\partial\Omega$ and unit outward normal vector η . The initial conditions u_0 and v_0 satisfy: $u_0, v_0 \in L^\infty(\Omega)$ such that $0 \leq u_0(x) \leq 1$ and $v_0(x) \geq 0$, for all $x \in \Omega$.

In the above model, the density of the cell-population and the chemoattractant (or repellent) concentration are represented by $u = u(x, t)$ and $v = v(x, t)$ respectively. Next, $a(u)$ is a density-dependent diffusion coefficient, and $\Lambda(x)$ is the diffusion tensor in a heterogeneous medium. Furthermore, the function $\chi(u)$ is the chemoattractant sensitivity, and $D(x)$ is the diffusion tensor for v . We assume that Λ and D are two bounded, uniformly positive symmetric tensors on Ω (i.e. $\forall \xi \neq 0, 0 < T_- |\xi|^2 \leq \langle T(x) \xi, \xi \rangle \leq T_+ |\xi|^2 < \infty$, $T = \Lambda$ or D). The function $f(u)$ describes cell proliferation and cell death, it is usually considered to follow the logistic growth with certain carrying capacity u_c which represents the maximum density that the environment can support (e.g. see [28]). The function $g(u, v)$ describes the rates of production and degradation of the chemoattractant; here, we assume it is the linear function given by

$$g(u, v) = \alpha u - \beta v, \quad \alpha, \beta \geq 0. \quad (2.4)$$

Painter and Hillen [29] introduced the mechanistic description of the volume-filling effect. In the volume-filling effect, it is assumed that particles have a finite volume and that cells cannot move into regions that are already filled by other cells. First, we give a brief derivation of the model below, where in addition we consider the elastic cell property; that is, we consider that the cells are deformable and elastic and can squeeze into openings.

The derivation of the model begins with a master equation for a continuous-time and discrete space-random walk introduced by Othmer and Stevens [30], that is

$$\frac{\partial u_i}{\partial t} = \mathcal{T}_{i-1}^+ u_{i-1} + \mathcal{T}_{i+1}^- u_{i+1} - (\mathcal{T}_i^+ + \mathcal{T}_i^-) u_i, \quad (2.5)$$

where \mathcal{T}_i^\pm are the transitional probabilities per unit of time for one-step jump to $i \pm 1$. Herein, we shall equate the probability distribution above with the cell density.

In the volume-filling approach, and in the context of chemotaxis, the probability of a cell making a jump is assumed to depend on additional factors, such as the external concentration of the chemotactic agent and the availability of space into which the cells can squeeze and move. Therefore, we consider in the transition probability the fact that the cells can detect a local gradient as well as squeeze into openings. We take

$$\mathcal{T}_i^\pm = q(u_{i\pm 1}) (\theta + \delta [\tau(v_{i\pm 1}) - \tau(v_i)]), \quad (2.6)$$

where $q(u)$ is a nonlinear function representing the squeezing probability of a cell finding space at its neighboring location, θ and δ are constants, and τ represents the mechanism of the signal detection of the chemical concentration (for more details see [29, 30]). It is assumed that only a finite number of cells, \bar{u} , can be accommodated at any site, and the function q is stipulated by the following condition:

$$q(\bar{u}) = 0 \quad \text{and} \quad 0 < q(u) \leq 1 \quad \text{for} \quad 0 \leq u < \bar{u}.$$

Clearly, a possible choice for the squeezing probability q is a nonlinear function (see [31] for more details), defined by

$$q(u) = \begin{cases} 1 - \left(\frac{u}{\bar{u}}\right)^\gamma, & 0 \leq u \leq \bar{u}, \\ 0, & u > \bar{u}, \end{cases} \quad (2.7)$$

where $\gamma \geq 1$ denotes the squeezing exponent. The case $\gamma = 1$ corresponds to the interpretation that cells are solid blocks. However, the cells are elastic and can squeeze into openings. Thus the squeezing probability should be considered as a nonlinear function.

Substituting equation (2.6) into the master equation (2.5) and assuming that the cell density can diffuse in a heterogeneous manner in the space we get the first equation of system (2.1), with the associated coefficients

$$a(u) = d_1 (q(u) - q'(u) u), \quad \chi(u) = \zeta u q(u), \quad (2.8)$$

where d_1 and ζ are two positive constants.

In this paper, we are interested in system (2.1) modeling the volume-filling chemotaxis process in the general case and for which we set $\bar{u} = 1$. Furthermore, we assume that the functions f and χ are continuous and satisfy:

$$f(0) = f(\bar{u}) = 0, \quad \chi(0) = \chi(\bar{u}) = 0. \quad (2.9)$$

3. CVFE discretization

Definition 3.1. (Primary and dual mesh)

Let Ω be an open bounded polygonal connected subset of \mathbb{R}^2 . A primary finite volume mesh of Ω is a triplet $(\mathcal{T}, \mathcal{E}, \mathcal{P})$, where \mathcal{T} is a family of disjoint open polygonal convex subsets of Ω called control volumes, \mathcal{E} is a family of subsets of $\bar{\Omega}$ contained in straight lines of \mathbb{R}^2 with strictly positive one-dimensional measure, called the edges of the control volumes, and \mathcal{P} is a family of points of Ω satisfying the following properties:

1. The closure of the union of all the control volumes is $\bar{\Omega}$, i.e. $\bar{\Omega} = \bigcup_{K \in \mathcal{T}} \bar{K}$.
2. For any $K \in \mathcal{T}$, there exists a subset \mathcal{E}_K of \mathcal{E} such that $\partial K = \bar{K} \setminus K = \bigcup_{\sigma \in \mathcal{E}_K} \bar{\sigma}$. Furthermore, $\mathcal{E} = \bigcup_{K \in \mathcal{T}} \mathcal{E}_K$.
3. There exists a Donald dual mesh $\mathcal{M} := \{M_i, i = 1, \dots, N_s\}$ associated with the triangulation $\mathcal{T} := \{K_i, i = 1, \dots, N_e\}$. For each triangle $K \in \mathcal{T}$, we connect the barycenter x_K with the midpoint of each edge $\sigma \in \mathcal{E}_K$, and thus the barycenter of $K \in \mathcal{T}$ is such that $x_K := \bigcap_{M \cap K \neq \emptyset} \partial M \in K$. We denote by x_M the center of each dual volume $M \in \mathcal{M}$ defined by $x_M := \bigcap_{K \cap M \neq \emptyset} \partial K \in M$. For each interface of the dual control volume M , we denote by $\sigma_{M,M'}^K := \partial M \cap \partial M' \cap K$ the line segment between the points x_K and the midpoint of the line segment $[x_M, x_{M'}]$ and let $\mathcal{L} := \{\sigma \in \partial M \setminus \partial \Omega, M \in \mathcal{M}\}$ be the set of all interior sides. Finally we denote by \mathcal{M}^{int} and \mathcal{M}^{ext} the set of all interior and all boundary dual volumes respectively. We refer to Fig. 1 for an illustration of the primal triangular mesh \mathcal{T} and its corresponding Donald dual mesh \mathcal{M} .

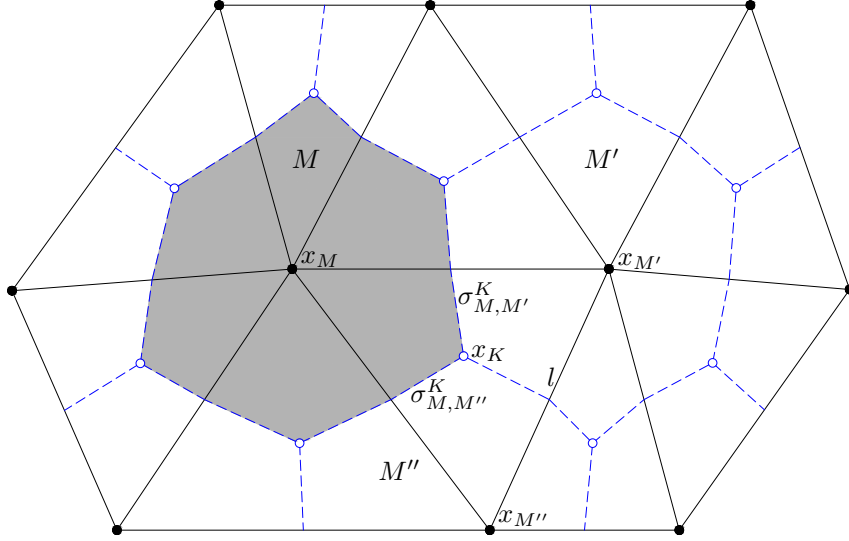


Figure 1: Donald dual mesh: control volumes, centers, interfaces.

In the sequel, we use the following notations. For any $M \in \mathcal{M}$, $|M|$ is the area of M . The set of neighbors of M is denoted by $\mathcal{N}(M) := \{M' \in \mathcal{M} / \exists \sigma \in \mathcal{L}, \bar{\sigma} = \bar{M} \cap \bar{M}'\}$, and we designate by $d_{M,M'}$ the distance between the centers of M and M' . We define the mesh size by $h := \text{size}(\mathcal{M}) = \sup_{M \in \mathcal{M}} \text{diam}(M)$ and make the following shape regularity assumption on the family of triangulations $\{\mathcal{T}_h\}_h$:

$$\text{There exists a positive constant } \kappa_{\mathcal{T}} \text{ such that: } \min_{K \in \mathcal{T}_h} \frac{|K|}{\text{diam}(K)^2} \geq \kappa_{\mathcal{T}}, \quad \forall h > 0. \quad (3.1)$$

For the time discretization, we do not impose any restriction on the time step, for that we consider a uniform time step $\Delta t \in (0, T)$. We take $N \in \mathbb{N}^*$ such that $N := \max \{n \in \mathbb{N} / n \Delta t < T\}$, and we denote $t_n = n \Delta t$, for $n \in \{0, \dots, N+1\}$, so that $t_0 = 0$, and $t_{N+1} = T$.

We define the following finite-dimensional spaces:

$$\begin{aligned}\mathcal{H}_h &:= \{\varphi_h \in C^0(\overline{\Omega}); \varphi_h|_K \in \mathbb{P}_1, \forall K \in \mathcal{T}_h\} \subset H^1(\Omega), \\ \mathcal{H}_h^0 &:= \{\varphi_h \in \mathcal{H}_h; \varphi_h(x_M) = 0, \forall M \in \mathcal{M}^{\text{ext}}\}.\end{aligned}$$

The canonical basis of \mathcal{H}_h is spanned by the shape functions $(\varphi_M)_{M \in \mathcal{M}}$, such that $\varphi_M(x_{M'}) = \delta_{M, M'}$ for all $M' \in \mathcal{M}_h$, δ being the Kronecker delta. The approximations in these spaces are conforming since $\mathcal{H}_h \subset H^1(\Omega)$. We equip \mathcal{H}_h with the semi-norm

$$\|u_h\|_{\mathcal{H}_h}^2 := \int_{\Omega} |\nabla u_h|^2 dx,$$

which becomes a norm on \mathcal{H}_h^0 .

The classical finite elements \mathbb{P}_1 associated to the vertex x_{M_i} ($i = 1, \dots, N_s$), where N_s is the total number of vertices, is defined by

$$\varphi_{M_i}(x_{M_j}) = \delta_{ij}, \text{ where } \varphi_{M_i} \text{ is continuous and piecewise } \mathbb{P}_1 \text{ per triangle.}$$

Let w_M^n be an expected approximation of $w(x_M, t_n)$, where $w \equiv u$ or v . Thus, the discrete unknowns are denoted by $\{w_M^n / M \in \mathcal{M}_h, n \in \{0, \dots, N+1\}\}$.

Definition 3.2. (Discrete functions). Using the values of (u_M^{n+1}, v_M^{n+1}) , $\forall M \in \mathcal{M}_h$ and $n \in \{0, \dots, N\}$, we determine two approximate solutions by means of the *control volume finite element scheme*:

- (i) A finite volume solution $(\tilde{u}_{h, \Delta t}; \tilde{v}_{h, \Delta t})$ defined as piecewise constant on the dual volumes in space and piecewise constant in time, such that:

$$\begin{aligned}(\tilde{u}_{h, \Delta t}(0, x), \tilde{v}_{h, \Delta t}(0, x)) &= (u_M^0, v_M^0) \quad \forall x \in \overset{\circ}{M}, M \in \mathcal{M}_h, \\ (\tilde{u}_{h, \Delta t}(t, x), \tilde{v}_{h, \Delta t}(t, x)) &= (u_M^{n+1}, v_M^{n+1}) \quad \forall x \in \overset{\circ}{M}, M \in \mathcal{M}_h, \forall t \in (t_n, t_{n+1}],\end{aligned}$$

where u_M^0 (resp. v_M^0) represents the mean value of the function u_0 (resp. v_0). The discrete space of these functions namely *discrete control volumes space* is denoted by $X_{h, \Delta t}$.

- (ii) A finite element solution $v_{h, \Delta t}$ as a function continuous and piecewise \mathbb{P}_1 per triangle in space and piecewise constant in time, such that:

$$\begin{aligned}v_{h, \Delta t}(0, x) &= v_h^0(x) \quad \forall x \in \Omega, \\ v_{h, \Delta t}(t, x) &= v_h^{n+1}(x) \quad \forall x \in \Omega, \forall t \in (t_n, t_{n+1}],\end{aligned}$$

where $v_h^{n+1}(x) := \sum_{M \in \mathcal{M}_h} v_M^{n+1} \varphi_M(x)$ and $v_h^0(x) := \sum_{M \in \mathcal{M}_h} v_M^0 \varphi_M(x)$. The discrete space of these functions namely *discrete finite elements space* is denoted by $\mathcal{H}_{h, \Delta t}$.

In the sequel, we use the nonlinear and continuous function $A : \mathbb{R} \longrightarrow \mathbb{R}$ defined by

$$A(u) = \int_0^u a(s) ds. \quad (3.2)$$

The function A is nonlinear, we denote by $A_{h,\Delta t} = A_h(u_{h,\Delta t})$ the corresponding finite element reconstruction in $\mathcal{H}_{h,\Delta t}$, and by $A(\tilde{u}_{h,\Delta t})$ the corresponding finite volume reconstruction in $X_{h,\Delta t}$. Specifically, we have

$$A_h(u_{h,\Delta t}(t, x)) = \sum_{M \in \mathcal{M}_h} A(u_M^{n+1}) \varphi_M(x), \quad \forall x \in \Omega, \forall t \in (t_n, t_{n+1}],$$

$$A(\tilde{u}_{h,\Delta t}(t, x)) = A(u_M^{n+1}), \quad \forall x \in \overset{\circ}{M}, M \in \mathcal{M}_h, \forall t \in (t_n, t_{n+1}].$$

3.1. CVFE scheme for the modified Keller-Segel model

In order to define a discretization for system (2.1), we integrate the equations of system (2.1) over the set $M \times [t_n, t_{n+1}]$ with $M \in \mathcal{M}_h$, then we use the Green–Gauss formula as well as the implicit order one discretization in time, we get

$$\begin{aligned} \int_M (u(t_{n+1}, x) - u(t_n, x)) \, dx - \sum_{\sigma \subset \partial M} \int_{t_n}^{t_{n+1}} \int_{\sigma} \Lambda \nabla A(u) \cdot \eta_{M,\sigma} \, dt \, d\sigma \\ + \sum_{\sigma \subset \partial M} \int_{t_n}^{t_{n+1}} \int_{\sigma} \chi(u) \Lambda \nabla v \cdot \eta_{M,\sigma} \, dt \, d\sigma = \int_{t_n}^{t_{n+1}} \int_M f(u) \, dt \, dx, \end{aligned} \quad (3.3)$$

$$\int_M (v(t_{n+1}, x) - v(t_n, x)) \, dx - \sum_{\sigma \subset \partial M} \int_{t_n}^{t_{n+1}} \int_{\sigma} D \nabla v \cdot \eta_{M,\sigma} \, dt \, d\sigma = \int_{t_n}^{t_{n+1}} \int_M g(u, v) \, dt \, dx,$$

where $\eta_{M,\sigma}$ is the unit normal vector outward to $\sigma \subset \partial M$.

We consider now an implicit Euler scheme in time, and thus the time evolution in the first equation of system (3.3) is approximated as

$$\int_M (u(t_{n+1}, x) - u(t_n, x)) \, dx \approx \int_M (\tilde{u}_{h,\Delta t}(t_{n+1}, x) - \tilde{u}_{h,\Delta t}(t_n, x)) \, dx = |M| (u_M^{n+1} - u_M^n).$$

Note that $f(u)$ is a nonlinear function. We denote by $f(\tilde{u}_{h,\Delta t})$ the corresponding piecewise constant reconstruction in $X_{h,\Delta t}$, then the reaction term is approximated as

$$\int_{t_n}^{t_{n+1}} \int_M f(u(t, x)) \, dt \, dx \approx \int_{t_n}^{t_{n+1}} \int_M f(\tilde{u}_{h,\Delta t}(t, x)) \, dt \, dx = |M| \Delta t f(u_M^{n+1}).$$

On the other hand, we distinguish two kinds of approximation in space. The first consists of considering the finite element approach to handle the diffusion term, and the second consists of using an upstream finite volume approach.

Let us focus on the discretization of the diffusion term of the first equation of system (3.3), we have

$$\sum_{\sigma \subset \partial M} \int_{t_n}^{t_{n+1}} \int_{\sigma} \Lambda \nabla A(u) \cdot \eta_{M,\sigma} \, dt \, d\sigma \approx \Delta t \sum_{\sigma \subset \partial M} \int_{\sigma} \Lambda \nabla A_h(u_{h,\Delta t}(t_{n+1}, x)) \cdot \eta_{M,\sigma} \, d\sigma. \quad (3.4)$$

The diffusion tensor $\Lambda(x)$ is taken constant per triangle, we denote by Λ_K the mean value of the function $\Lambda(x)$ over the triangle $K \in \mathcal{T}_h$, then one rewrites the right hand side of equation (3.4) as

$$\begin{aligned} \Delta t \sum_{K, K \cap M \neq \emptyset} \sum_{\sigma \subset \partial M \cap K} \Lambda_K \nabla A_h(u_{h,\Delta t}(t_{n+1}, x)) \Big|_K \cdot \eta_{M,\sigma} |\sigma| \\ = \Delta t \sum_{K, K \cap M \neq \emptyset} \frac{1}{2} \nabla A_h(u_{h,\Delta t}(t_{n+1}, x)) \Big|_K \cdot {}^t \Lambda_K \eta_{K,l} |l| \end{aligned} \quad (3.5)$$

where $l \in \mathcal{E}_K$ such that $M \cap l = \emptyset$, and $\eta_{K,l}$ denotes the unit normal vector outward to the edge l . For the transition between the first and the second line in approximation (3.5), we have used a geometric property, that is

$$\sum_{\sigma \subset \partial M \cap K} \eta_{M,\sigma} |\sigma| = \frac{1}{2} \eta_{K,l} |l|, \quad \forall K \in \mathcal{T}_h \text{ such that } K \cap M \neq \emptyset.$$

According to the definition of the approximate function $\nabla A_h(u_{h,\Delta t})$, one has

$$\nabla A_h(u_{h,\Delta t}(t_{n+1}, x)) \Big|_K = \sum_{M \in \mathcal{M}_h} A(u_M^{n+1}) \nabla \varphi_M(x) \Big|_K. \quad (3.6)$$

Note that, the \mathbb{P}_1 -finite element bases are expressed in barycentric coordinates, thus

$$\sum_{M', M' \cap K \neq \emptyset} \varphi_{M'}(x) \Big|_K = 1, \text{ and } \sum_{M', M' \cap K \neq \emptyset} \nabla \varphi_{M'}(x) \Big|_K = 0,$$

consequently, we have

$$\nabla A_h(u_{h,\Delta t}(t_{n+1}, x)) \Big|_K = \sum_{M', M' \cap K \neq \emptyset} (A(u_{M'}^{n+1}) - A(u_M^{n+1})) \nabla \varphi_{M'} \Big|_K. \quad (3.7)$$

We note that, for a given $K \in \mathcal{T}_h$, we have

$$\nabla \varphi_M \Big|_K = \frac{-|l|}{2|K|} \eta_{K,l}, \quad \forall M \in \mathcal{M}_h \text{ such that } M \cap K \neq \emptyset. \quad (3.8)$$

Let us now introduce the transmissibility coefficient between M and M' defined by

$$\Lambda_{M,M'}^K = - \int_K \Lambda(x) \nabla \varphi_M(x) \cdot \nabla \varphi_{M'}(x) \, dx. \quad (3.9)$$

As a consequence of (3.8)–(3.9), one has

$$\sum_{\sigma \subset \partial M} \int_{t_n}^{t_{n+1}} \int_{\sigma} \Lambda \nabla A(u) \cdot \eta_{M,\sigma} \, dt \, d\sigma \approx \Delta t \sum_{K, M \cap K \neq \emptyset} \sum_{M', M' \cap K \neq \emptyset} \Lambda_{M,M'}^K (A(u_{M'}^{n+1}) - A(u_M^{n+1})).$$

Next, we have to approximate the convective term in the first equation of system (3.3). For that, we consider an upstream finite volume scheme according to the normal component of the gradient of the chemoattractant v on the interfaces. So,

$$\begin{aligned} \sum_{\sigma \subset \partial M} \int_{t_n}^{t_{n+1}} \int_{\sigma} \chi(u) \Lambda \nabla v \cdot \eta_{M,\sigma} \, dt \, d\sigma \\ \approx \Delta t \sum_{K, K \cap M \neq \emptyset} \sum_{\sigma \subset \partial M \cap K} \int_{\sigma} \Lambda(x) \chi(\tilde{u}_{h,\Delta t}(t_{n+1}, x)) \nabla v_{h,\Delta t}(t_{n+1}, x) \cdot \eta_{M,\sigma} \, d\sigma. \end{aligned}$$

In order to approximate the convective flux on each interface, let us firstly introduce an example of approximation in the case where the function χ is nondecreasing. For that, we consider the interface $\sigma_{M,M'}^K$, and write

$$\int_{\sigma_{M,M'}^K} \chi(\tilde{u}_{h,\Delta t}(t_{n+1}, x)) \Lambda \nabla v_{h,\Delta t}(t_{n+1}, x) \cdot \eta_{\sigma} \, d\sigma \approx \begin{cases} |\sigma_{M,M'}^K| \chi(u_M^{n+1}) \, dV_{M,M'}^K, & \text{if } dV_{M,M'}^K \geq 0, \\ |\sigma_{M,M'}^K| \chi(u_{M'}^{n+1}) \, dV_{M,M'}^K, & \text{if } dV_{M,M'}^K \leq 0, \end{cases}$$

where $dV_{M,M'}^K$ represents an approximation of the gradient of v on the interface $\sigma_{M,M'}^K$

$$dV_{M,M'}^K = \sum_{M'', M'' \cap K \neq \emptyset} v_{M''}^{n+1} \nabla \varphi_{M''}|_K \cdot {}^t \Lambda_K \eta_{M,M'}^K. \quad (3.10)$$

Thus, the convective term is approximated as

$$\begin{aligned} & \sum_{\sigma \in \partial M} \int_{t_n}^{t_{n+1}} \int_{\sigma} \chi(u) \Lambda \nabla v \cdot \eta_{M,\sigma} dt d\sigma \\ & \approx \begin{cases} \Delta t \sum_{K, M \cap K \neq \emptyset} \sum_{M', M' \cap K \neq \emptyset} \chi(u_M^{n+1}) \Lambda_{M,M'}^K (v_{M'}^{n+1} - v_M^{n+1}), & \text{if } dV_{M,M'}^K \geq 0, \\ \Delta t \sum_{K, M \cap K \neq \emptyset} \sum_{M', M' \cap K \neq \emptyset} \chi(u_{M'}^{n+1}) \Lambda_{M,M'}^K (v_{M'}^{n+1} - v_M^{n+1}), & \text{if } dV_{M,M'}^K \leq 0, \end{cases} \end{aligned}$$

where $\Lambda_{M,M'}^K$ represents the transmissibility coefficient between M and M' , given by equation (3.9).

In the general case, we use numerical convection flux functions G of arguments $(a, b, c) \in \mathbb{R}^3$ which are required to satisfy the properties:

$$\left\{ \begin{array}{l} \text{(a) } G(\cdot, b, c) \text{ is nondecreasing for all } b, c \in \mathbb{R}, \\ \text{and } G(a, \cdot, c) \text{ is nonincreasing for all } a, c \in \mathbb{R}; \\ \text{(b) } G(a, b, c) = -G(b, a, -c) \text{ for all } a, b, c \in \mathbb{R}; \\ \text{(c) } G(a, a, c) = \chi(a) c \text{ for all } a, c \in \mathbb{R}; \\ \text{(d) there exists } C > 0 \text{ such that} \\ \quad \forall a, b, c \in \mathbb{R} \quad |G(a, b, c)| \leq C(|a| + |b|)|c|; \\ \text{(e) there exists a modulus of continuity } \omega : \mathbb{R}^+ \rightarrow \mathbb{R}^+ \text{ such that} \\ \quad \forall a, b, a', b', c \in \mathbb{R} \quad |G(a, b, c) - G(a', b', c)| \leq |c| \omega(|a - a'| + |b - b'|). \end{array} \right. \quad (3.11)$$

In our context, one possibility to construct a numerical flux G satisfying conditions (3.11) is to split χ into the nondecreasing part χ_{\uparrow} and the nonincreasing part χ_{\downarrow} :

$$\chi_{\uparrow}(z) := \int_0^z (\chi'(s))^+ ds, \quad \chi_{\downarrow}(z) := - \int_0^z (\chi'(s))^- ds.$$

Herein, $s^+ = \max(s, 0)$ and $s^- = \max(-s, 0)$. Then we take

$$G(a, b, c) = c^+ (\chi_{\uparrow}(a) + \chi_{\downarrow}(b)) - c^- (\chi_{\uparrow}(b) + \chi_{\downarrow}(a)). \quad (3.12)$$

Notice that in the case χ has a unique local (and global) maximum at the point $\tilde{u} \in (0, 1)$, we have

$$\chi_{\uparrow}(z) = \chi(\min\{z, \tilde{u}\}) \quad \text{and} \quad \chi_{\downarrow}(z) = \chi(\max\{z, \tilde{u}\}) - \chi(\tilde{u}).$$

For the discretization of the second equation of system (3.3), we define the transmissibility coefficient $D_{M,M'}^K$ by

$$D_{M,M'}^K = \int_K D(x) \nabla \varphi_M(x) \cdot \nabla \varphi_{M'}(x) dx. \quad (3.13)$$

then we follow the same lines as for the discretization of the first equation.

We are now in position to discretize problem (2.1)–(2.3). We denote by \mathcal{D}_h a discretization of

Q_T , which consists of a primary finite element mesh \mathcal{T}_h and a Donald dual mesh \mathcal{M}_h of Ω and a time step $\Delta t > 0$.

A *control volume finite element scheme* for the discretization of problem (2.1)–(2.3) is given by the following set of equations: for all $M \in \mathcal{M}_h$,

$$u_M^0 = \frac{1}{|M|} \int_M u_0(x) dx, \quad v_M^0 = \frac{1}{|M|} \int_M v_0(x) dx, \quad (3.14)$$

and for all $M \in \mathcal{M}_h$ and all $n \in \{0, \dots, N\}$,

$$\begin{aligned} |M| \frac{u_M^{n+1} - u_M^n}{\Delta t} - \sum_{K, M \cap K \neq \emptyset} \sum_{M', M' \cap K \neq \emptyset} \Lambda_{M, M'}^K (A(u_{M'}^{n+1}) - A(u_M^{n+1})) \\ + \sum_{K, M \cap K \neq \emptyset} \sum_{M', M' \cap K \neq \emptyset} |\sigma_{M, M'}^K| G(u_M^{n+1}, u_{M'}^{n+1}; dV_{M, M'}^K) = |M| f(u_M^{n+1}), \end{aligned} \quad (3.15)$$

$$|M| \frac{v_M^{n+1} - v_M^n}{\Delta t} - \sum_{K, M \cap K \neq \emptyset} \sum_{M', M' \cap K \neq \emptyset} D_{M, M'}^K (v_{M'}^{n+1} - v_M^{n+1}) = |M| g(u_M^n, v_M^{n+1}), \quad (3.16)$$

we recall that the unknowns are $U = (u_M^{n+1})_{M \in \mathcal{M}_h}$ and $V = (v_M^{n+1})_{M \in \mathcal{M}_h}$, $n \in \{0, \dots, N\}$, and that $dV_{M, M'}^K$ is defined in equation (3.10), and the transmissibility coefficients $\Lambda_{M, M'}^K$ and $D_{M, M'}^K$ are given by (3.9) and (3.13) respectively. Notice that the discrete zero-flux boundary conditions are implicitly contained in equations (3.15)–(3.16). The contribution of $\partial\Omega \cap \partial M$ to the approximation of $\int_{\partial M} D \nabla v \cdot \eta d\sigma$ and $\int_{\partial M} \Lambda (\nabla A(u) - \chi(u) \nabla v) \cdot \eta d\sigma$ is zero, in compliance with equation (2.2).

In this paper, we assume that the transmissibility coefficients $\Lambda_{M, M'}^K$ and $D_{M, M'}^K$ are nonnegative:

$$\Lambda_{M, M'}^K \geq 0 \text{ and } D_{M, M'}^K \geq 0, \quad \forall M, M' \in \mathcal{M}_h, \forall K \in \mathcal{T}_h. \quad (3.17)$$

4. A priori analysis of discrete solutions

In this section, we prove the discrete maximum principle, then we establish the *a priori* estimates necessary to prove the existence of a solution to the discrete problem (3.14)–(3.16) and the convergence towards the weak solution. In the sequel, we denote by C a “generic” constant, which need not have the same value through the proofs.

4.1. Nonnegativity of v_h , confinement of u_h

Lemma 4.1. *Let $(u_M^n, v_M^n)_{M \in \mathcal{M}_h, n \in \{0, \dots, N+1\}}$ be a solution of the CVFE scheme (3.14)–(3.16). Under the nonnegativity of transmissibility coefficients assumption (3.17), we have for all $M \in \mathcal{M}_h$, and all $n \in \{0, \dots, N+1\}$, $0 \leq u_M^n \leq 1$ and $0 \leq v_M^n$. Moreover, there exists a positive constant $\rho = \|v_0\|_\infty + \alpha T$, such that $v_M^n \leq \rho$, for all $n \in \{0, \dots, N+1\}$.*

Proof. Let us show by induction on n that for all $M \in \mathcal{M}_h$, $u_M^n \geq 0$. The claim is true for $n = 0$. We argue by induction that for all $M \in \mathcal{M}_h$, the claim is true up to order n . Consider a dual control volume M such that $u_M^{n+1} = \min \{u_{M'}^{n+1}\}_{M' \in \mathcal{M}_h}$, we want to show that $u_M^{n+1} \geq 0$. We consider equation (3.15) corresponding to the aforementioned dual volume M , reorganize the

summation over the edges and multiply it by $-(u_M^{n+1})^-$ where for all real r , $r = r^+ - r^-$ with $r^+ = \max(r, 0)$ and $r^- = \max(-r, 0)$. This yields

$$\begin{aligned} & -|M| \frac{u_M^{n+1} - u_M^n}{\Delta t} (u_M^{n+1})^- + \sum_{\sigma_{M,M'}^K \subset \partial M} \Lambda_{M,M'}^K (A(u_{M'}^{n+1}) - A(u_M^{n+1})) (u_M^{n+1})^- \\ & - \sum_{\sigma_{M,M'}^K \subset \partial M} |\sigma_{M,M'}^K| G(u_M^{n+1}, u_{M'}^{n+1}; dV_{M,M'}^K) (u_M^{n+1})^- = -f(u_M^{n+1}) (u_M^{n+1})^-. \end{aligned} \quad (4.1)$$

Here, we use the extension by zero of the function f for $u \leq 0$ since $f(0) = 0$, then the right hand side of equation (4.1) is equal to zero.

The function A is nondecreasing then $A(u_{M'}^{n+1}) - A(u_M^{n+1}) \geq 0$ and the assumption $\Lambda_{M,M'}^K \geq 0$ implies that

$$\sum_{\sigma_{M,M'}^K \subset \partial M} \Lambda_{M,M'}^K (A(u_{M'}^{n+1}) - A(u_M^{n+1})) (u_M^{n+1})^- \geq 0.$$

From the assumptions on the numerical flux G , the function G is nonincreasing with respect to the second variable and using the extension of χ (recall that $\chi(u) = 0$ for $u \leq 0$), we get

$$\begin{aligned} G(u_M^{n+1}, u_{M'}^{n+1}; dV_{M,M'}^K) (u_M^{n+1})^- & \leq G(u_M^{n+1}, u_{M'}^{n+1}; dV_{M,M'}^K) (u_M^{n+1})^- \\ & = dV_{M,M'}^K \chi(u_M^{n+1}) (u_M^{n+1})^- = 0. \end{aligned}$$

Using the identity $u_M^{n+1} = (u_M^{n+1})^+ - (u_M^{n+1})^-$ and the nonnegativity of u_K^n , we deduce from equation (4.1) that $(u_M^{n+1})^- = 0$. According to the choice of the dual control volume M , then $\min\{u_{M'}^{n+1}\}_{M' \in \mathcal{M}_h}$ is nonnegative; this ends the proof of the first claim.

The proof of nonnegativity of v_M^n , $M \in \mathcal{M}_h$, $n \in \{0, \dots, N+1\}$, follows the same lines as for the proof for the nonnegativity of u_M^n , since $-g(u_M^n, v_M^{n+1})(u_M^{n+1})^- = -\alpha |M| u_M^n (v_M^{n+1})^- + \beta |M| v_M^{n+1} (v_M^{n+1})^- \leq 0$.

In order to prove (by induction) that $u_M^{n+1} \leq 1$, we take M such that $u_M^{n+1} = \max(u_{M'}^{n+1})_{M' \in \mathcal{M}_h}$.

Next, multiplying equation (3.15) by $(u_M^{n+1} - 1)^+$, with the same arguments as in the above proof, and using the extension by zero of the functions f and χ for $u \geq 1$. We find that $(u_M^{n+1} - 1)^+ = 0$ and thus $u_M^{n+1} \leq 1$ for all $M \in \mathcal{M}_h$.

Let us now focus on the last claim concerning the existence of a constant ρ such that $v_M^n \leq \rho$. We set $\rho_n := \|v_0\|_\infty + n\alpha\Delta t$, and suppose that $v_M^n \leq \rho_n$, $\forall M \in \mathcal{M}_h$ (the claim holds for $n = 0$). We want to show that $v_M^{n+1} \leq \rho_{n+1}$, for that we take the dual volume M such that $v_M^{n+1} = \max\{v_{M'}^{n+1}\}_{M' \in \mathcal{M}_h}$. Using scheme (3.16), one has

$$\begin{aligned} |M| \frac{v_M^{n+1} - \rho_{n+1}}{\Delta t} + |M| \beta v_M^{n+1} - \sum_{K, M \cap K \neq \emptyset} \sum_{M', M' \cap K \neq \emptyset} D_{M,M'}^K (v_{M'}^{n+1} - v_M^{n+1}) \\ = \alpha |M| (u_M^n - 1) + |M| \frac{v_M^n - \rho_n}{\Delta t}. \end{aligned} \quad (4.2)$$

Multiplying equation (4.2) by $(v_M^{n+1} - \rho_{n+1})^+$, one can deduce that $v_M^{n+1} \leq \rho_{n+1} \leq \rho$, for all $n \in \{0, \dots, N\}$. This ends the proof of the lemma. \square

4.2. A priori estimates

Proposition 4.2. *Let $(u_M^{n+1}, v_M^{n+1})_{M \in \mathcal{M}_h, n \in \{0, \dots, N\}}$, be a solution of the control volume finite element scheme (3.14)–(3.16). Under assumption (3.1) and assumption (3.17), there exists a*

constant $C > 0$, depending on Ω , T , $\|v_0\|_\infty$, α , and on the constant in (3.11)(d) such that

$$\begin{aligned} \sum_{n=0}^N \Delta t \sum_{M \in \mathcal{M}_h} \sum_{\sigma_{M,M'}^K \subset \partial M} \Lambda_{M,M'}^K |A(u_M^{n+1}) - A(u_{M'}^{n+1})|^2 \\ + \sum_{n=0}^N \Delta t \sum_{M \in \mathcal{M}_h} \sum_{\sigma_{M,M'}^K \subset \partial M} D_{M,M'}^K |v_M^{n+1} - v_{M'}^{n+1}|^2 \leq C, \end{aligned} \quad (4.3)$$

and consequently, for all $A_h^{n+1} = \sum_{M \in \mathcal{M}_h} A(u_M^{n+1}) \varphi_M \in \mathcal{H}_h$, and all $v_h^{n+1} = \sum_{M \in \mathcal{M}_h} v_M^{n+1} \varphi_M \in \mathcal{H}_h$,

$$\sum_{n=0}^N \Delta t \|v_h^{n+1}\|_{\mathcal{H}_h}^2 \leq C, \quad (4.4)$$

and

$$\sum_{n=0}^N \Delta t \|A_h(u_h^{n+1})\|_{\mathcal{H}_h}^2 \leq C. \quad (4.5)$$

Proof. We multiply equation (3.15) (resp. equation (3.16)) by $A(u_M^{n+1})$ (resp. by v_M^{n+1}), and perform a sum over $M \in \mathcal{M}_h$ and $n \in \{0, \dots, N\}$. This yields

$$E_{1,1} + E_{1,2} + E_{1,3} = E_{1,4} \quad \text{and} \quad E_{2,1} + E_{2,2} = E_{2,3},$$

where

$$\begin{aligned} E_{1,1} &= \sum_{n=0}^N \sum_{M \in \mathcal{M}_h} |M| (u_M^{n+1} - u_M^n) A(u_M^{n+1}), \quad E_{2,1} = \sum_{n=0}^N \sum_{M \in \mathcal{M}_h} |M| (v_M^{n+1} - v_M^n) v_M^{n+1}, \\ E_{1,2} &= \sum_{n=0}^N \Delta t \sum_{M \in \mathcal{M}_h} \sum_{\sigma_{M,M'}^K \subset \partial M} \Lambda_{M,M'}^K (A(u_M^{n+1}) - A(u_{M'}^{n+1})) A(u_M^{n+1}), \\ E_{2,2} &= \sum_{n=0}^N \Delta t \sum_{M \in \mathcal{M}_h} \sum_{\sigma_{M,M'}^K \subset \partial M} D_{M,M'}^K (v_M^{n+1} - v_{M'}^{n+1}) v_M^{n+1}, \\ E_{1,3} &= \sum_{n=0}^N \Delta t \sum_{M \in \mathcal{M}_h} \sum_{\sigma_{M,M'}^K \subset \partial M} |\sigma_{M,M'}^K| G(u_M^{n+1}, u_{M'}^{n+1}; dV_{M,M'}^K) A(u_M^{n+1}), \\ E_{1,4} &= \sum_{n=0}^N \Delta t \sum_{M \in \mathcal{M}_h} |M| f(u_M^{n+1}) A(u_M^{n+1}), \quad E_{2,3} = \sum_{n=0}^N \Delta t \sum_{M \in \mathcal{M}_h} |M| (\alpha u_M^n - \beta v_M^{n+1}) v_M^{n+1}. \end{aligned}$$

Let $\mathcal{B}(s) = \int_0^s A(r) \, dr$; we have $\mathcal{B}''(s) = a(s) \geq 0$, so that \mathcal{B} is convex. From the convexity of \mathcal{B} , we have the following inequality

$$\forall a, b \in \mathbb{R} \quad (a - b) A(a) \geq \mathcal{B}(a) - \mathcal{B}(b).$$

Using this inequality for the term $E_{1,1}$, we obtain

$$E_{1,1} \geq \sum_{n=0}^N \sum_{M \in \mathcal{M}_h} |M| (\mathcal{B}(u_M^{n+1}) - \mathcal{B}(u_M^n)) = \sum_{M \in \mathcal{M}_h} |M| (\mathcal{B}(u_M^{N+1}) - \mathcal{B}(u_M^0)).$$

Next, for the diffusive term $E_{1,2}$, we reorganize the sum over edges. Then, we have

$$\begin{aligned} E_{1,2} &= \sum_{n=0}^N \Delta t \sum_{\sigma_{M,M'}^K \in \mathcal{E}_h} \Lambda_{M,M'}^K (A(u_M^{n+1}) - A(u_{M'}^{n+1}))^2 \\ &= \frac{1}{2} \sum_{n=0}^N \Delta t \sum_{M \in \mathcal{M}_h} \sum_{\sigma_{M,M'}^K \subset \partial M} \Lambda_{M,M'}^K (A(u_M^{n+1}) - A(u_{M'}^{n+1}))^2. \end{aligned}$$

We estimate the convective term $E_{1,3}$, and also gather by edges, one gets

$$\begin{aligned} E_{1,3} &= \sum_{n=0}^N \Delta t \sum_{M \in \mathcal{M}_h} \sum_{\sigma_{M,M'}^K \subset \partial M} |\sigma_{M,M'}^K| G(u_M^{n+1}, u_{M'}^{n+1}; dV_{M,M'}^K) A(u_M^{n+1}) \\ &= \sum_{n=0}^N \Delta t \sum_{\sigma_{M,M'}^K \in \mathcal{E}_h} |\sigma_{M,M'}^K| G(u_M^{n+1}, u_{M'}^{n+1}; dV_{M,M'}^K) (A(u_M^{n+1}) - A(u_{M'}^{n+1})). \end{aligned}$$

Using the definition of the function G , the assumption (3.11)(d) and the boundedness of u_M^{n+1} , and applying the weighted Young inequality, one has

$$|E_{1,3}| \leq \sum_{n=0}^N \Delta t \sum_{\sigma_{M,M'}^K \in \mathcal{E}_h} |\sigma_{M,M'}^K| |G(u_M^{n+1}, u_{M'}^{n+1}; dV_{M,M'}^K) (A(u_M^{n+1}) - A(u_{M'}^{n+1}))| \leq E_{1,3}^1 + E_{1,3}^2,$$

where

$$\begin{aligned} E_{1,3}^1 &= \frac{1}{4} \sum_{n=0}^N \Delta t \sum_{M \in \mathcal{M}_h} \sum_{\sigma_{M,M'}^K \subset \partial M} \Lambda_{M,M'}^K |A(u_M^{n+1}) - A(u_{M'}^{n+1})|^2, \\ E_{1,3}^2 &= C \sum_{n=0}^N \Delta t \sum_{M \in \mathcal{M}_h} \sum_{\sigma_{M,M'}^K \subset \partial M} |G(u_M^{n+1}, u_{M'}^{n+1}; dV_{M,M'}^K) \sigma_{M,M'}^K|^2 \\ &\leq C \sum_{n=0}^N \Delta t \sum_{M \in \mathcal{M}_h} \sum_{\sigma_{M,M'}^K \subset \partial M} |dV_{M,M'}^K|^2 |\sigma_{M,M'}^K|^2. \end{aligned}$$

On the other hand, using the definition (3.10) of $dV_{M,M'}^K$, we get

$$|dV_{M,M'}^K| |\sigma_{M,M'}^K| \leq C \sum_{M'', M'' \cap K \neq \emptyset} |v_{M''}^{n+1} - v_M^{n+1}| |\nabla \varphi_{M''}|_K |\sigma_{M,M'}^K|.$$

Thanks to the shape regularity assumption (3.1), one can deduce that $|\nabla \varphi_{M''}|_K \times |\sigma_{M,M'}^K| \leq C$. As a consequence,

$$\begin{aligned}
|E_{1,3}| &\leq \frac{1}{4} \sum_{n=0}^N \Delta t \sum_{M \in \mathcal{M}_h} \sum_{\sigma_{M,M'}^K \subset \partial M} \Lambda_{M,M'}^K |A(u_M^{n+1}) - A(u_{M'}^{n+1})|^2 \\
&\quad + C \sum_{n=0}^N \Delta t \sum_{M \in \mathcal{M}_h} \sum_{\sigma_{M,M'}^K \subset \partial M} D_{M,M'}^K |v_{M'}^{n+1} - v_M^{n+1}|^2.
\end{aligned}$$

The last estimation for the reactive term is given using definition (2.4) of g and the boundedness of u_M^{n+1} , v_M^{n+1} , and f . Then

$$\begin{aligned}
E_{2,3} &= \sum_{n=0}^N \Delta t \sum_{M \in \mathcal{M}_h} |M| \left(\alpha u_M^n v_M^{n+1} - \beta (v_M^{n+1})^2 \right) \leq \sum_{n=0}^N \Delta t \sum_{M \in \mathcal{M}_h} \alpha |M| u_M^n v_M^{n+1} \leq \alpha \rho T |\Omega|. \\
E_{1,4} &= \sum_{n=0}^N \Delta t \sum_{M \in \mathcal{M}_h} |M| f(u_M^{n+1}) A(u_M^{n+1}) \leq CT |\Omega|.
\end{aligned}$$

Collecting the previous inequalities, one can deduce that there exists a constant $C > 0$, independent of h and Δt , such that

$$\begin{aligned}
&\sum_{n=0}^N \Delta t \sum_{M \in \mathcal{M}_h} \sum_{\sigma_{M,M'}^K \subset \partial M} \Lambda_{M,M'}^K |A(u_M^{n+1}) - A(u_{M'}^{n+1})|^2 \\
&\quad + \sum_{n=0}^N \Delta t \sum_{M \in \mathcal{M}_h} \sum_{\sigma_{M,M'}^K \subset \partial M} D_{M,M'}^K |v_M^{n+1} - v_{M'}^{n+1}|^2 \leq C.
\end{aligned}$$

Let us focus on estimate (4.5), we denote by D_K , $K \in \mathcal{T}_h$ the mean value of the function D over the triangle K , then using the previous estimates as well as the assumptions on the diffusion tensor D , one has

$$\begin{aligned}
C &\geq \sum_{n=0}^N \Delta t \sum_{M \in \mathcal{M}_h} \sum_{\sigma_{M,M'}^K \subset \partial M} D_{M,M'}^K |v_M^{n+1} - v_{M'}^{n+1}|^2 \\
&= 2 \sum_{n=0}^N \Delta t \sum_{M \in \mathcal{M}_h} v_M^{n+1} \sum_{\sigma_{M,M'}^K \subset \partial M} D_{M,M'}^K (v_M^{n+1} - v_{M'}^{n+1}) \\
&= 2 \sum_{n=0}^N \Delta t \sum_{M \in \mathcal{M}_h} \sum_{K \in \mathcal{T}_h} |K| v_M^{n+1} \nabla \varphi_M|_K \cdot {}^t D_K \sum_{M' \in \mathcal{M}_h} v_{M'}^{n+1} \nabla \varphi_{M'}|_K \\
&= \sum_{n=0}^N \Delta t \sum_{K \in \mathcal{T}_h} |K| D_K \left(\sum_{M \in \mathcal{M}_h} v_M^{n+1} \nabla \varphi_M|_K \right) \cdot \left(\sum_{M' \in \mathcal{M}_h} v_{M'}^{n+1} \nabla \varphi_{M'}|_K \right) \\
&= \sum_{n=0}^N \Delta t \sum_{K \in \mathcal{T}_h} \int_K D(x) \nabla v_h^{n+1} \cdot \nabla v_h^{n+1} dx \geq 2D_- \sum_{n=0}^N \Delta t \int_{\Omega} |\nabla v_h^{n+1}|^2 dx.
\end{aligned}$$

In the same manner, we obtain estimate (4.4). This ends the proof of the **Proposition 4.2**. \square

4.3. Existence of a discrete solution

The existence of a solution to the *control volume finite element scheme* is given by the following proposition.

Proposition 4.3. *Under the shape regularity assumption (3.1) and the nonnegativity assumption (3.17), there exists at least one solution $(u_M^{n+1}, v_M^{n+1})_{(M,n) \in \mathcal{M} \times \llbracket 0 \dots N \rrbracket}$ for the discrete problem (3.14)–(3.16).*

The proof is provided with the help of the Brower fixed point theorem (e.g. see [32]). This method is used in [13] and it is easy to adopt the proof in our case, thus we omit it.

5. Compactness estimates on discrete solutions

In this section, we derive estimates on differences of time and space translates necessary to prove the relative compactness property of the sequence of approximate solutions using Kolmogorov's theorem. Under the shape regularity assumption (3.1) and the nonnegativity of the transmissibility coefficients assumption (3.17), we give the time and space translate estimates for $A(\tilde{u}_{h,\Delta t})$ and $\tilde{v}_{h,\Delta t}$ given by **Definition 3.2**.

Lemma 5.1. *Under assumption (3.1) and assumption (3.17), there exists a positive constant $C > 0$ depending on Ω , T , α , u_0 and v_0 such that*

$$\iint_{\Omega' \times (0,T)} |\tilde{w}_{h,\Delta t}(t, x+y) - \tilde{w}_{h,\Delta t}(t, x)|^2 dt dx \leq C |y| (|y| + 2h), \quad \tilde{w}_{h,\Delta t} = A(\tilde{u}_{h,\Delta t}), \tilde{v}_{h,\Delta t}, \quad (5.1)$$

for all $y \in \mathbb{R}^2$ with $\Omega' = \{x \in \Omega, [x, x+y] \subset \Omega\}$, and

$$\iint_{\Omega \times (0, T-\tau)} |\tilde{w}_{h,\Delta t}(t+\tau, x) - \tilde{w}_{h,\Delta t}(t, x)|^2 dt dx \leq C (\tau + \Delta t), \quad \tilde{w}_{h,\Delta t} = A(\tilde{u}_{h,\Delta t}), \tilde{v}_{h,\Delta t}, \quad (5.2)$$

for all $\tau \in (0, T)$.

Proof. The proof of estimate (5.1) follows the same lines as in [14, Lemma 3.3, p.44] and using the shape regularity assumption (3.1). For the sake of brevity, we do not provide it here. Let us now focus on estimate (5.2). Let $\tau \in (0, T)$ and $t \in (0, T - \tau)$. We define

$$\Upsilon(t) := \int_{\Omega} |A(\tilde{u}_{h,\Delta t})(t+\tau, x) - A(\tilde{u}_{h,\Delta t})(t, x)|^2 dx.$$

Set $n_0(t) = \lfloor t/\Delta t \rfloor$ and $n_1(t) = \lfloor (t+\tau)/\Delta t \rfloor$, where $\lfloor x \rfloor = n$ for $x \in [n, n+1)$, $n \in \mathbb{N}$. Since A is nondecreasing, we have the following inequality

$$\iint_{\Omega \times (0, T-\tau)} |A(\tilde{u}_{h,\Delta t})(t+\tau, x) - A(\tilde{u}_{h,\Delta t})(t, x)|^2 dt dx \leq C \int_0^{T-\tau} \Upsilon(t) dt,$$

where, for almost every $t \in (0, T - \tau)$,

$$\Upsilon(t) = \sum_{M \in \mathcal{M}_h} |M| \left(A(u_M^{n_1(t)}) - A(u_M^{n_0(t)}) \right) (u_M^{n_1(t)} - u_M^{n_0(t)}).$$

Note that the function $\Upsilon(t)$ may be written as

$$\Upsilon(t) = \sum_{M \in \mathcal{M}_h} \left(A(u_M^{n_1(t)}) - A(u_M^{n_0(t)}) \right) \sum_{n=0}^{N-1} \chi_n(t, t+\tau) |M| (u_M^{n+1} - u_M^n), \quad (5.3)$$

where, χ_n is the characteristic function defined by

$$\chi_n(t, t + \tau) = \begin{cases} 1 & \text{if } (n+1)\Delta t \in (t, t + \tau], \\ 0 & \text{if } (n+1)\Delta t \notin (t, t + \tau]. \end{cases}$$

In equation (5.3), the order of the summation between n and M is changed and the scheme (3.15) is used. Hence,

$$\begin{aligned} \Upsilon(t) = & \Delta t \sum_{n=0}^{N-1} \chi_n(t, t + \tau) \sum_{M \in \mathcal{M}_h} \left(A(u_M^{n_1(t)}) - A(u_M^{n_0(t)}) \right) \times \\ & \left(\sum_{\sigma_{M,M'}^K \subset \partial M} \Lambda_{M,M'}^K (A(u_{M'}^{n+1}) - A(u_M^{n+1})) - \sum_{\sigma_{M,M'}^K \subset \partial M} |\sigma_{M,M'}^K| G(u_M^{n+1}, u_{M'}^{n+1}; dV_{M,M'}^K) \right) \\ & + \Delta t \sum_{n=0}^{N-1} \chi_n(t, t + \tau) \sum_{M \in \mathcal{M}_h} \left(A(u_M^{n_1(t)}) - A(u_M^{n_0(t)}) \right) \times |M| f(u_M^{n+1}). \end{aligned}$$

We write $\Upsilon(t) = \Delta t \sum_{n=0}^{N-1} \chi_n(t, t + \tau) (\Upsilon_1(t) + \Upsilon_2(t) + \Upsilon_3(t))$, where

$$\begin{aligned} \Upsilon_1(t) &:= \sum_{M \in \mathcal{M}_h} \sum_{\sigma_{M,M'}^K \subset \partial M} \Lambda_{M,M'}^K \left(A(u_M^{n_1(t)}) - A(u_M^{n_0(t)}) \right) (A(u_{M'}^{n+1}) - A(u_M^{n+1})), \\ \Upsilon_2(t) &:= \sum_{M \in \mathcal{M}_h} \sum_{\sigma_{M,M'}^K \subset \partial M} |\sigma_{M,M'}^K| \left(A(u_M^{n_0(t)}) - A(u_M^{n_1(t)}) \right) G(u_M^{n+1}, u_{M'}^{n+1}; dV_{M,M'}^K), \\ \Upsilon_3(t) &:= \sum_{M \in \mathcal{M}_h} |M| \left(A(u_M^{n_1(t)}) - A(u_M^{n_0(t)}) \right) f(u_M^{n+1}). \end{aligned}$$

It's easy to see that

$$\sum_{n=0}^{N-1} \Delta t \int_0^{T-\tau} \chi_n(t, t + \tau) \Upsilon_3(t) dt \leq C(\tau + \Delta t).$$

For the first term, note that gathering by edges, using the basic triangle inequality, one has

$$\begin{aligned} \Upsilon_1(t) \leq & \frac{1}{2} \left(\sum_{M \in \mathcal{M}_h} \sum_{\sigma_{M,M'}^K \subset \partial M} \Lambda_{M,M'}^K (A(u_{M'}^{n+1}) - A(u_M^{n+1}))^2 \right. \\ & + \frac{1}{2} \sum_{M \in \mathcal{M}_h} \sum_{\sigma_{M,M'}^K \subset \partial M} \Lambda_{M,M'}^K \left| A(u_M^{n_1(t)}) - A(u_{M'}^{n_1(t)}) \right|^2 \\ & \left. + \frac{1}{2} \sum_{M \in \mathcal{M}_h} \sum_{\sigma_{M,M'}^K \subset \partial M} \Lambda_{M,M'}^K \left| A(u_M^{n_0(t)}) - A(u_{M'}^{n_0(t)}) \right|^2 \right). \end{aligned}$$

Using the estimates (4.3), this implies that there exists a constant $C > 0$ independent of τ and h , such that $\sum_{n=0}^{N-1} \Delta t \int_0^{T-\tau} \chi_n(t, t + \tau) \Upsilon_1(t) dt \leq C(\tau + \Delta t)$. Finally, applying the previous

arguments, gathering by edges, and using each of the definition of G and the assumptions on it, we get

$$\begin{aligned} \Upsilon_2(t) dt \leq & \frac{C}{2} \left(\sum_{M \in \mathcal{M}_h} \sum_{\sigma_{M,M'}^K \subset \partial M} \left(\left| A(u_M^{n_1(t)}) - A(u_{M'}^{n_1(t)}) \right|^2 + |v_M^{n+1} - v_{M'}^{n+1}|^2 \right) \right. \\ & \left. + \sum_{M \in \mathcal{M}_h} \sum_{\sigma_{M,M'}^K \subset \partial M} \left(\left| A(u_M^{n_0(t)}) - A(u_{M'}^{n_0(t)}) \right|^2 + |v_M^{n+1} - v_{M'}^{n+1}|^2 \right) \right). \end{aligned}$$

We use estimates (4.3) to deduce that

$$\sum_{n=0}^{N-1} \Delta t \int_0^{T-\tau} \chi_n(t, t+\tau) \Upsilon_2(t) dt \leq C(\tau + \Delta t).$$

Consequently, we obtain

$$\begin{aligned} \int_0^{T-\tau} \Upsilon(t) dt \leq & \sum_{n=0}^{N-1} \Delta t \int_0^{T-\tau} \chi_n(t, t+\tau) (\Upsilon_1(t) + \Upsilon_3(t)) dt \\ & + \sum_{n=0}^{N-1} \Delta t \int_0^{T-\tau} \chi_n(t, t+\tau) \Upsilon_2(t) dt \leq C(\tau + \Delta t), \end{aligned}$$

for some constant C independent of τ and h . The proof of (5.2) for $\tilde{w}_{h,\Delta t} = \tilde{v}_{h,\Delta t}$ follows in a similar manner. This concludes the proof of the lemma. \square

6. Convergence of the CVFE scheme

We can prove the main result of this section. Specifically, we have the following lemmas.

Lemma 6.1. *The sequences $(A(\tilde{u}_{h,\Delta t}) - A_h(u_{h,\Delta t}))_{h,\Delta t}$ and $(\tilde{v}_{h,\Delta t} - v_{h,\Delta t})_{h,\Delta t}$ converge strongly to zero in $L^2(Q_T)$ as $h \rightarrow 0$.*

Proof. Using the definition of the basis functions of the finite dimensional space \mathcal{H}_h , we have for all $M \in \mathcal{M}_h$ and all $K \in \mathcal{T}_h$ such that $M \cap K \neq \emptyset$

$$\begin{aligned} |A(\tilde{u}_{h,\Delta t}) - A_h(u_{h,\Delta t})|^2 &= |A(\tilde{u}_{h,\Delta t})(t_{n+1}, x_M) - A_h(u_{h,\Delta t})(t_{n+1}, x)|^2 \\ &= |\nabla A_h(u_{h,\Delta t})(t_{n+1}, x) \cdot (x_M - x)|^2, \quad \forall x \in K \cap M \end{aligned}$$

where x_M is the center of the dual volume $M \in \mathcal{M}_h$.

Using estimate (4.5), one obtains

$$\begin{aligned} \|A(\tilde{u}_{h,\Delta t}) - A_h(u_{h,\Delta t})\|_{L^2(Q_T)}^2 &= \sum_{n=0}^N \Delta t \sum_{K \in \mathcal{T}_h} \sum_{M, M \cap K \neq \emptyset} \int_{K \cap M} |\nabla A_h(u_{h,\Delta t})(t_{n+1}, x) \cdot (x_M - x)|^2 \\ &\leq h^2 \sum_{n=0}^N \Delta t \sum_{K \in \mathcal{T}_h} \sum_{M, M \cap K \neq \emptyset} |K \cap M| |\nabla A_h(u_h^{n+1})|_K|^2 \\ &\leq h^2 \sum_{n=0}^N \Delta t \|A_h(u_h^{n+1})\|_{\mathcal{H}_h}^2 \leq Ch^2, \end{aligned}$$

consequently, we have $\|A(\tilde{u}_{h,\Delta t}) - A_h(u_{h,\Delta t})\|_{L^2(Q_T)} \rightarrow 0$ as $h \rightarrow 0$. In the same manner, we prove that $\|\tilde{v}_{h,\Delta t} - v_{h,\Delta t}\|_{L^2(Q_T)} \rightarrow 0$ as $h \rightarrow 0$. \square

Lemma 6.2. *(Convergence of the scheme). Under the shape regularity assumption (3.1) and the nonnegativity of the transmissibility coefficients assumption (3.17), there exists a sequence $(h_m)_{m \in \mathbb{N}}$, $h_m \rightarrow 0$ as $m \rightarrow \infty$, and functions u, v defined in Q_T such that $0 \leq u \leq 1$, both $A(u)$ and v belong to $L^2(0, T; H^1(\Omega))$, and*

$$A_{h_m}(u_{h_m}) \rightarrow A(u) \text{ and } v_{h_m} \rightarrow v \text{ a.e. in } Q_T \text{ and strongly in } L^p(Q_T) \text{ for all } p < +\infty$$

Proof. Let us set $\tilde{A}_{h,\Delta t} := A(\tilde{u}_{h,\Delta t})$ in Q_T and $\tilde{A}_{h,\Delta t} := 0$ in $\mathbb{R}^3 \setminus Q_T$. Thanks to Proposition 4.2 and Lemma 4.1, one has $(\tilde{A}_{h,\Delta t}) \subset L^\infty(\mathbb{R}^3) \cap L^2(\mathbb{R}^3)$. In order to verify the assumptions of Kolmogorov's compactness criterion, see [14, theorem 3.9, p:93], we note that the following inequality is verified for any $\eta \in \mathbb{R}^2$ and $\tau \in \mathbb{R}$,

$$\begin{aligned} \left\| \tilde{A}_{h,\Delta t}(\cdot + \eta, \cdot + \tau) - \tilde{A}_{h,\Delta t}(\cdot, \cdot) \right\|_{L^2(\mathbb{R}^3)} &\leq \left\| \tilde{A}_{h,\Delta t}(\cdot + \eta, \cdot) - \tilde{A}_{h,\Delta t}(\cdot, \cdot) \right\|_{L^2(\mathbb{R}^3)} \\ &\quad + \left\| \tilde{A}_{h,\Delta t}(\cdot, \cdot + \tau) - \tilde{A}_{h,\Delta t}(\cdot, \cdot) \right\|_{L^2(\mathbb{R}^3)}, \end{aligned}$$

Now, using Lemma 5.1, we deduce that $\left\| \tilde{A}_{h,\Delta t}(\cdot + \eta, \cdot + \tau) - \tilde{A}_{h,\Delta t}(\cdot, \cdot) \right\|_{L^2(\mathbb{R}^{2+1})} \rightarrow 0$, as $\eta \rightarrow 0$ and $\tau \rightarrow 0$. This yields the compactness of the sequence $(\tilde{A}_{h,\Delta t})$ in $L^2(\Omega)$.

Thus, there exists a subsequence, still denoted by $(\tilde{A}_{h,\Delta t})$, and there exists $A^* \in L^2(Q_T)$ such that

$$A(\tilde{u}_{h,\Delta t}) \rightarrow A^* \text{ strongly in } L^2(Q_T).$$

Furthermore, as A is strictly monotone, there exists a unique u such that $A(u) = A^*$. Since A^{-1} is well defined and continuous, then applying the L^∞ bound on u_h and the dominated convergence theorem to $\tilde{u}_{h,\Delta t} = A^{-1}(A(\tilde{u}_{h,\Delta t}))$, we get

$$\tilde{u}_{h,\Delta t} \rightarrow u \text{ a.e. in } Q_T \text{ and strongly in } L^p(Q_T) \text{ for } p < +\infty.$$

According to Lemma 6.1, the sequences $(A(\tilde{u}_{h,\Delta t}))_{h,\Delta t}$ and $(A_h(u_{h,\Delta t}))_{h,\Delta t}$ have the same limit, as a consequence

$$A_h(u_{h,\Delta t}) \rightarrow A(u) \text{ strongly in } L^2(Q_T) \text{ and a.e. in } Q_T.$$

Similarly, translate estimates (5.1)–(5.2), the L^∞ bound on $v_{h,\Delta t}$ in Lemma 4.1, and Lemma 6.1 ensure that, up to extraction of a subsequence,

$$v_{h,\Delta t} \rightarrow v \text{ a.e. in } Q_T \text{ and strongly in } L^p(Q_T) \text{ for } p < +\infty.$$

This ends the proof of the lemma. \square

It remains to be shown that the limit functions u and v constitute a weak solution of the continuous system. For this, let $\psi \in \mathcal{D}([0, T] \times \bar{\Omega})$ be a test function and denote by $\psi_M^n := \psi(t_n, x_M)$ for all $M \in \mathcal{M}_h$ and $n \in \{0, \dots, N+1\}$. Multiply equation (3.15) by $\Delta t \psi_M^{n+1}$, and sum up over $M \in \mathcal{M}_h$ and $n \in \{0, \dots, N\}$. This yields

$$S_1^h + S_2^h + S_3^h = S_4^h$$

$$\begin{aligned}
S_1^h &:= \sum_{n=0}^N \sum_{M \in \mathcal{M}_h} |M| (u_M^{n+1} - u_M^n) \psi_M^{n+1}, \quad S_4^h := \sum_{n=0}^N \Delta t \sum_{M \in \mathcal{M}_h} |M| f(u_M^{n+1}) \psi_M^{n+1}, \\
S_2^h &:= \sum_{n=0}^N \Delta t \sum_{M \in \mathcal{M}_h} \sum_{\sigma_{M,M'}^K \subset \partial M} G(u_M^{n+1}, u_{M'}^{n+1}; dV_{M,M'}^K) \psi_M^{n+1} |\sigma_{M,M'}^K|, \\
S_3^h &:= \sum_{n=0}^N \Delta t \sum_{M \in \mathcal{M}_h} \sum_{\sigma_{M,M'}^K \subset \partial M} \Lambda_{M,M'}^K (A(u_M^{n+1}) - A(u_{M'}^{n+1})) \psi_M^{n+1}.
\end{aligned}$$

Performing a summation by parts in time and keeping in mind that $\psi_M^{N+1} = 0$ for all $M \in \mathcal{M}_h$, we obtain

$$\begin{aligned}
S_1^h &= \sum_{n=0}^N \sum_{M \in \mathcal{M}_h} |M| u_M^{n+1} \psi_M^{n+1} - \sum_{n=0}^N \sum_{M \in \mathcal{M}_h} |M| u_M^n \psi_M^{n+1} \\
&= - \sum_{n=0}^N \sum_{M \in \mathcal{M}_h} \Delta t |M| u_M^n \frac{\psi_M^{n+1} - \psi_M^n}{\Delta t} - \sum_{M \in \mathcal{M}_h} |M| u_M^0 \psi_M^0 \\
&= - \sum_{n=0}^N \sum_{M \in \mathcal{M}_h} \int_{t_n}^{t_{n+1}} \int_M \tilde{u}_{h,\Delta t}(x, t) \partial_t \psi(x_M, t) dt dx - \sum_{M \in \mathcal{M}_h} \int_M \tilde{u}_{h,\Delta t}(x, 0) \psi(x_M, 0) dx.
\end{aligned}$$

Taking into account the assumptions on the data and using the Lebesgue theorem, it follows that

$$S_1^h \xrightarrow{h, \Delta t \rightarrow 0} - \int_0^T \int_{\Omega} u \partial_t \psi dt dx - \int_{\Omega} u_0 \psi(\cdot, 0) dx.$$

On the other hand, for the convergence of the third term S_3^h , we note that

$$\begin{aligned}
S_3^h &= \sum_{n=0}^N \Delta t \left[\sum_{M \in \mathcal{M}_h} \sum_{\sigma_{M,M'}^K \subset \partial M} \Lambda_{M,M'}^K A(u_M^{n+1}) \psi_M^{n+1} - \sum_{M \in \mathcal{M}_h} \sum_{\sigma_{M,M'}^K \subset \partial M} \Lambda_{M,M'}^K A(u_{M'}^{n+1}) \psi_M^{n+1} \right] \\
&= - \sum_{n=0}^N \Delta t \sum_{M \in \mathcal{M}_h} A(u_M^{n+1}) \sum_{\sigma_{M,M'}^K \subset \partial M} \Lambda_{M,M'}^K (\psi_{M'}^{n+1} - \psi_M^{n+1}) \\
&= - \sum_{n=0}^N \sum_{M \in \mathcal{M}_h} \Delta t A(u_M^{n+1}) \sum_{K \cap M \neq \emptyset} \sum_{\sigma_{M,M'}^K \subset \partial M \cap K} \nabla \psi^{n+1} \Big|_K \cdot {}^t \Lambda_K \eta_{M,\sigma} |\sigma| \\
&= - \sum_{n=0}^N \sum_{M \in \mathcal{M}_h} \Delta t A(u_M^{n+1}) \sum_{\sigma_{M,M'}^K \subset \partial M} \nabla \psi^{n+1} \Big|_K \cdot {}^t \Lambda_K \eta_{M,\sigma} |\sigma| \\
&= - \sum_{n=0}^N \sum_{M \in \mathcal{M}_h} \Delta t A(u_M^{n+1}) \int_{\partial M} \Lambda \nabla \psi^{n+1} \cdot \eta d\sigma \\
&= - \sum_{n=0}^N \sum_{M \in \mathcal{M}_h} \int_{t_n}^{t_{n+1}} \int_M A(\tilde{u}_{h,\Delta t}(t, x)) \operatorname{div}(\Lambda \nabla \psi) dt dx \\
&\xrightarrow{h, \Delta t \rightarrow 0} - \iint_{Q_T} A(u) \operatorname{div}(\Lambda \nabla \psi) dt dx = \iint_{Q_T} \nabla A(u) \cdot \Lambda \nabla \psi dt dx.
\end{aligned}$$

It remains to show that

$$\lim_{h, \Delta t \rightarrow \infty} S_2^h = - \int_0^T \int_{\Omega} \Lambda(x) \chi(u) \nabla v \cdot \nabla \psi \, dt \, dx. \quad (6.1)$$

For the convergence of S_2^h , we note that gathering by edges (thanks to the consistency of the fluxes, see (3.11)(b)), we find

$$S_2^h = -\frac{1}{2} \sum_{n=0}^N \Delta t \sum_{M \in \mathcal{M}_h} \sum_{\sigma_{M,M'}^K \subset \partial M} G\left(u_M^{n+1}, u_{M'}^{n+1}; dV_{M,M'}^{n+1}\right) (\psi_{M'}^{n+1} - \psi_M^{n+1}) |\sigma_{M,M'}^K|.$$

For each triplet of neighbors M, M' , and M'' pick for $u_{K,\min}^{n+1}$ the quantity defined by

$$u_{K,\min}^{n+1} = \min_{M \in \mathcal{M}, M \cap K \neq \emptyset} \{u_M^{n+1}\}$$

Set

$$S_2^{h,*} := \sum_{n=0}^N \Delta t \sum_{M \in \mathcal{M}_h} \sum_{K, K \cap M \neq \emptyset} \sum_{M', M' \cap K \neq \emptyset} \chi\left(u_{K,\min}^{n+1}\right) \psi_M^{n+1} dV_{M,M'}^{n+1} |\sigma_{M,M'}^K|.$$

We have

$$\begin{aligned} S_2^{h,*} &= - \sum_{n=0}^N \Delta t \sum_{M \in \mathcal{M}_h} \sum_{K, K \cap M \neq \emptyset} \chi\left(u_{K,\min}^{n+1}\right) |K| \Lambda_K \psi_M^{n+1} \nabla \varphi_M|_K \cdot \left(\sum_{M'', M'' \cap K \neq \emptyset} v_{M''}^{n+1} \nabla \varphi_{M''}|_K \right) \\ &= - \sum_{n=0}^N \Delta t \sum_{K \in \mathcal{T}_h} |K| \chi\left(u_{K,\min}^{n+1}\right) \Lambda_K \left(\sum_{M, M \cap K \neq \emptyset} \psi_M^{n+1} \nabla \varphi_M|_K \right) \cdot \left(\sum_{M'', M'' \cap K \neq \emptyset} v_{M''}^{n+1} \nabla \varphi_{M''}|_K \right). \end{aligned}$$

Introduce $\bar{u}_h, \underline{u}_h$ defined by

$$\bar{u}_h|_{(t_n, t_{n+1}] \times K} := \max_{M, M \cap K \neq \emptyset} \{u_M^{n+1}\}, \quad \underline{u}_h|_{(t_n, t_{n+1}] \times K} := \min_{M, M \cap K \neq \emptyset} \{u_M^{n+1}\}.$$

Consequently, we obtain

$$S_2^{h,*} = - \sum_{n=0}^N \Delta t \sum_{K \in \mathcal{T}_h} \int_K \chi(\underline{u}_h) \Lambda_K \nabla v_{h,\Delta t}^{n+1} \cdot (\nabla \psi)_h^{n+1} \, dx = - \int_{Q_T} \chi(\underline{u}_h) \Lambda \nabla v_{h,\Delta t} \cdot (\nabla \psi)_{h,\Delta t} \, dt \, dx$$

Next, we show that

$$\lim_{h \rightarrow 0} |S_2^h - S_2^{h,*}| = 0. \quad (6.2)$$

To do this, we begin by showing that $|\underline{u}_h - \bar{u}_h| \rightarrow 0$ a.e. in Q_T .

By the monotonicity of A and thanks to the estimate (4.3), we have

$$\begin{aligned} \int_0^T \int_{\Omega} |A(\bar{u}_h) - A(\underline{u}_h)|^2 \, dt \, dx &\leq \sum_{n=0}^N \Delta t \sum_{M \in \mathcal{M}_h} \sum_{\sigma_{M,M'}^K \subset \partial M} |K| |A(u_{M'}^{n+1}) - A(u_M^{n+1})|^2 \\ &\leq C h^2 \sum_{n=0}^N \Delta t \sum_{M \in \mathcal{M}_h} \sum_{\sigma_{M,M'}^K \subset \partial M} \Lambda_{M,M'}^K |A(u_{M'}^{n+1}) - A(u_M^{n+1})|^2 \leq C h^2. \end{aligned}$$

Since A^{-1} is continuous, up to extraction of another subsequence, we deduce

$$|\bar{u}_h - \underline{u}_h| \rightarrow 0 \text{ a.e. in } Q_T. \quad (6.3)$$

In addition, $\underline{u}_h \leq \tilde{u}_{h,\Delta t} \leq \bar{u}_h$; moreover, by Lemma 6.2, $\tilde{u}_{h,\Delta t} \rightarrow u$ a.e. in Q_T . Thus we see that $\chi(\underline{u}_h) \rightarrow \chi(u)$ a.e. in Q_T and in $L^p(Q_T)$, for $p < +\infty$. Using Lemma 6.2 again, the strong convergence of $(\nabla \psi)_h$ towards $\nabla \psi$, and the weak convergence in $L^2(Q_T)$ of $\nabla v_{h,\Delta t}$ towards ∇v , we conclude that

$$\lim_{h \rightarrow 0} S_2^{h,*} = - \int_0^T \int_{\Omega} \chi(u) \Lambda \nabla v \cdot \nabla \psi \, dt \, dx.$$

To prove (6.2), we remark that

$$\begin{aligned} |G(u_M^{n+1}, u_{M'}^{n+1}, dV_{M,M'}^{n+1}) - \chi(u_{K,min}^{n+1}) dV_{M,M'}^{n+1}| \\ = |G(u_M^{n+1}, u_{M'}^{n+1}, dV_{M,M'}^{n+1}) - G(u_{K,min}^{n+1}, u_{K,min}^{n+1}, dV_{M,M'}^{n+1})| \\ \leq |dV_{M,M'}^{n+1}| \omega(2|u_{M'}^{n+1} - u_M^{n+1}|). \end{aligned}$$

Consequently,

$$|S_2^h - S_2^{h,*}| \leq \int_0^T \int_{\Omega} \omega(2|\bar{u}_h - \underline{u}_h|) |\nabla v_{h,\Delta t} \cdot (\nabla \psi)_{h,\Delta t}| \, dt \, dx.$$

Applying the Cauchy-Schwarz inequality, and the convergence (6.2), we establish (6.1).

Finally, we note that it is easy to see that $S_4^h \xrightarrow{h,\Delta t \rightarrow 0} \int_{Q_T} f(u) \psi \, dt \, dx$.

7. Numerical simulation in two-dimensional space

In this section, we exhibit various two-dimensional numerical results provided by scheme (3.14)–(3.16) for the capture of spatial patterns for model (2.1) discussed in Section 2. Newton's algorithm is used to approach the solution U^{n+1} of the nonlinear system defined by equation (3.15), this algorithm is coupled with a bigradient method to solve the linear systems arising from the Newton algorithm as well as the linear system given by equation (3.16). Unless stated otherwise, throughout this section, we consider that the cell density is initially set as a spatially small random perturbation around the homogeneous steady state, and we assume zero-flux boundary conditions. The simulations are performed on an unstructured triangular mesh of the space domain $\Omega = (0, 10) \times (0, 10)$. We suppose that the species cells follow the logistic growth $f(u) = \mu u(1 - u/u_c)$, where μ is the *intrinsic growth rate*, and u_c is the *carrying capacity* of the population. Production term $g(u, v)$, squeezing probability $q(u)$, cell diffusivity $a(u)$, and chemotactic sensitivity $\chi(u)$ are given by (2.4), (2.7), and (2.8) respectively.

The pattern formation for model (2.1) with the associated functions mentioned above has been established in [31] using Turing's principle and the linear stability analysis, where the diffusion tensor is considered to be proportional to the identity matrix and the numerical simulations are carried on a one-dimensional space, while in [33], the same analysis is provided whereas the numerical simulations for the capture of spatial patterns are presented on a two-dimensional domain, and using the standard finite volume scheme.

The nontrivial uniform steady state of system (2.1) is given by $(u_s, v_s) = (u_c, \alpha u_c / \beta)$, and through the pattern formation analysis provided in [31, 33], the instability region of this steady state is determined by the following condition:

$$\mu + \beta a(u_c) - \alpha \chi(u_c) < -2\sqrt{\mu \beta a(u_c)}. \quad (7.1)$$

In order to verify the effectiveness of the proposed scheme, we consider three tests for the capture of spatio-temporal patterns for model (2.1) with different diffusion tensors. For each test, we choose a set of parameters, such that the instability condition (7.1) is satisfied. We fix $d_1 = 0.25$, $u_c = 0.25$, $\bar{u} = 1.0$, $\mu = 0.5$, $\alpha = 10.0$, $\beta = 10.0$, $\zeta = 20$, and $\gamma = 3$. On the other hand, and in the definition of the numerical flux function G defined by (3.11), we take

$$\chi_{\uparrow}(z) = \chi(\min\{z, \tilde{u}\}) \text{ and } \chi_{\downarrow}(z) = \chi(\max\{z, \tilde{u}\}) - \chi(\tilde{u})$$

where $\tilde{u} = \frac{\bar{u}}{\sqrt[\gamma]{\gamma+1}}$. Finally, we consider a small time step $\Delta t = 0.005$ and a nonuniform primary

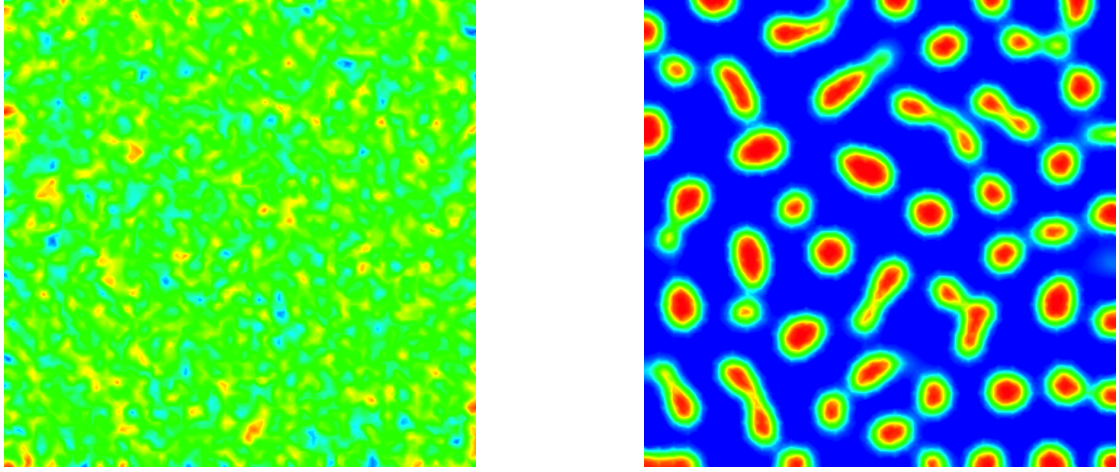


Figure 2: Pattern formation for the full chemotaxis model (2.1) on a 2-D domain $\Omega = (0, 10) \times (0, 10)$ at time $t = 0$ s with $0 \leq u \leq 1$ (*left*) and at time $t = 0.55$ s with $3.10^{-3} \leq u \leq 0.99$ (*right*).

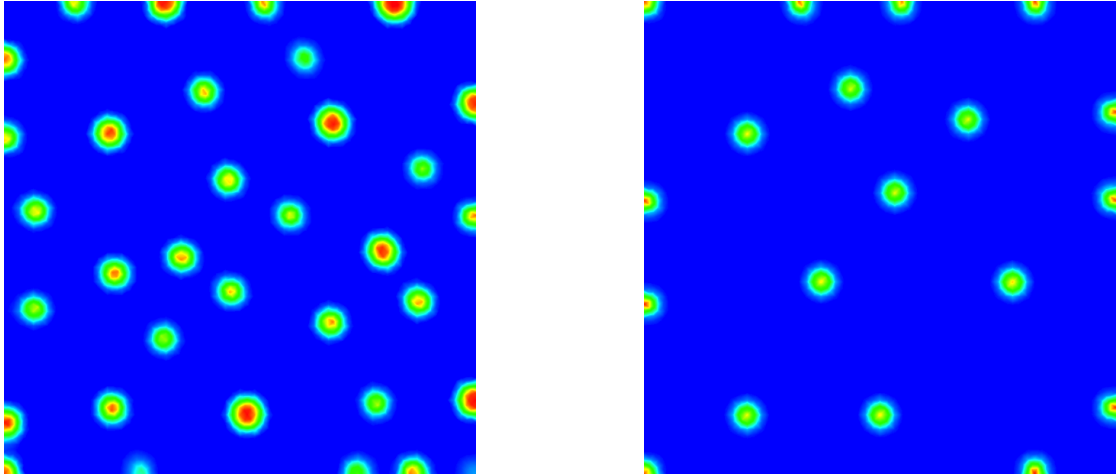


Figure 3: Pattern formation for the full chemotaxis model (2.1) at time $t = 2.35$ s with $1.9 \times 10^{-4} \leq u \leq 0.98$ (*left*) and at time $t = 40$ s with $3.9 \times 10^{-3} \leq u \leq 0.832$ (*right*). The red dots (or rods) represent the cell aggregation where cell density is higher than that of the blue area.

mesh with small refinement consisting of 14 336 triangles. Thus, the associated Donald dual mesh consists of 7297 dual volumes.

Test 1 (Isotropic case). Here, we establish the generation of spatial patterns for the volume-filling chemotaxis model (2.1) with homogeneous diffusion tensors. In this test, we take $\Lambda(x) = D(x) = I_2(x)$ and initially the chemical concentration is set to be a constant equal to v_s .

Figures 2–3 show for different moments, the pattern formation for model (2.1) with identity diffusion tensors. We see that the random distribution of the cell density leads to a merging process in all directions of the space at $t = 0.55s$, which continues for $t = 2.35s$ then it stops when the time $t \geq 20.75s$, and new stationary spot patterns appear as shown at $t = 40s$.

Time evolution of the cell density. Here we consider the time evolution of the cell density at fixed points in the right snapshot of Figure 3. Indeed, we want to show that the cell density stabilizes at a certain moment; hence, we prove that the volume-filling chemotaxis model (2.1) generates stationary spatial patterns. Figure 4 shows the evolution of the cell density with respect to the time at point $P_1(5.25; 6)$ in the red line, at point $P_2(5; 1.25)$ in the green line, and at point $P_3(4.35; 8.1)$ in the blue line. We observe that the cell density at these points increases and then decreases with response to the gradient of the chemoattractant which plays an essential role to stop the aggregation of the cells. Next, the cell density stabilizes for all points when t is greater or equal to 13s. We note that the same results are obtained for the other spot patterns; however, for the sake of brevity, they are not provided here.

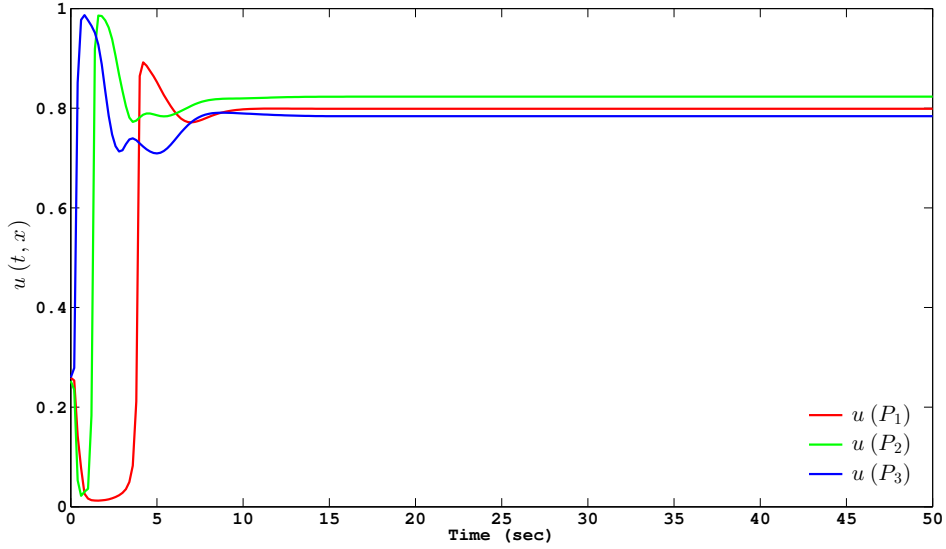


Figure 4: Evolution of the cell density with respect to the time at three different points: $P_1(5.25; 6)$ in the red line, $P_2(5; 1.25)$ in the green line, $P_3(4.35; 8.1)$ in the blue line.

Test 2 (Anisotropic case). In this test, we take anisotropic diffusion tensors of the form $\begin{bmatrix} 1 & 0 \\ 0 & \xi \end{bmatrix}$. We investigate the pattern formation for model (2.1) and consider that the particles diffuse more rapidly in the x -axis direction than the y -axis direction, for that we take $\xi = 0.5$. We pick up snapshots for the pattern formation at the same moments as for the isotropic case.

Figures 5–6 show the evolution of spatial patterns for model (2.1) for different time moments. We observe that we have the same results as before (same patterning, and emerging process),

except that more spot patterns are obtained and they are stretched in the horizontal direction as shown in the last snapshot in figure 6.

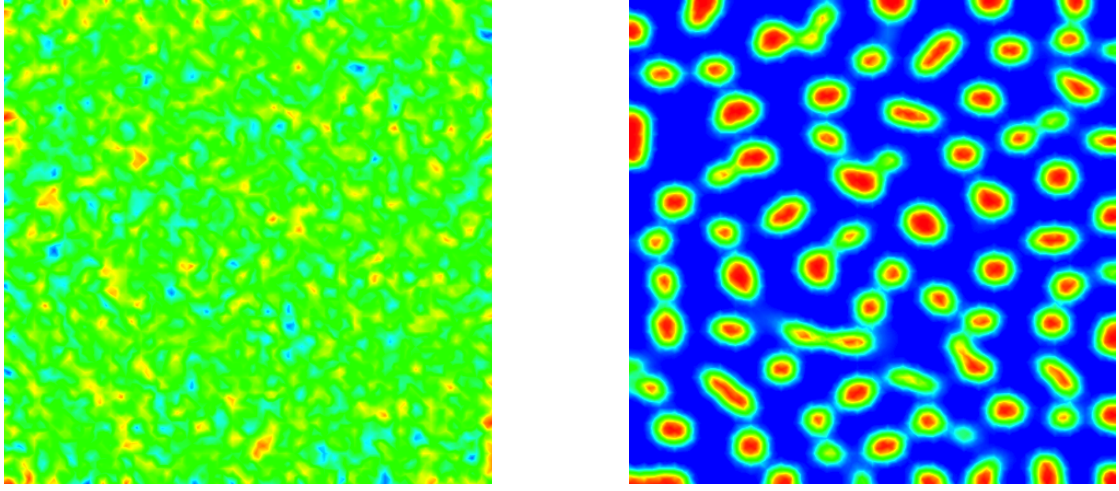


Figure 5: Pattern formation for the full chemotaxis model (2.1) on a 2-D domain $\Omega = (0, 10) \times (0, 10)$ at time $t = 0$ s with $0 \leq u \leq 1$ (*left*) and at time $t = 0.55$ s with $4.10^{-3} \leq u \leq 0.98$ (*right*).

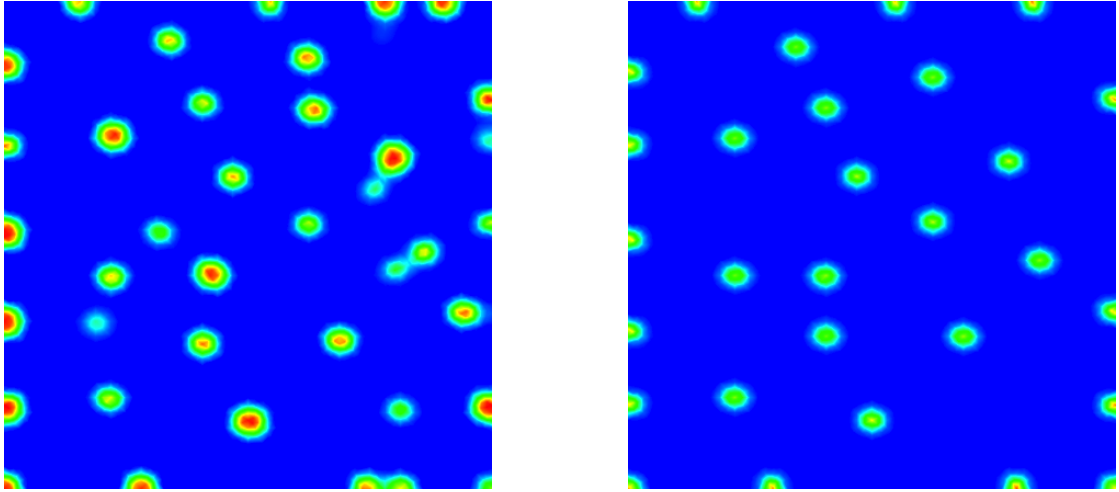


Figure 6: Pattern formation for the full chemotaxis model (2.1) at time $t = 2.35$ s with $3.2 \times 10^{-4} \leq u \leq 0.98$ (*left*) and at time $t = 40$ s with $4 \times 10^{-3} \leq u \leq 0.827$ (*right*).

The time evolution for the last plot in figure 6 for different spots is given in figure 7. It shows that the stationary spot patterns are obtained when $t \geq 23.5$ s.

Test 3 (Heterogeneous anisotropic case). In this test, we decompose the domain Ω into two regions Ω_1 and Ω_2 , where $\Omega_1 = (0, 10) \times (0, 5]$ and $\Omega_2 = (0, 10) \times (5, 10)$. Moreover, we

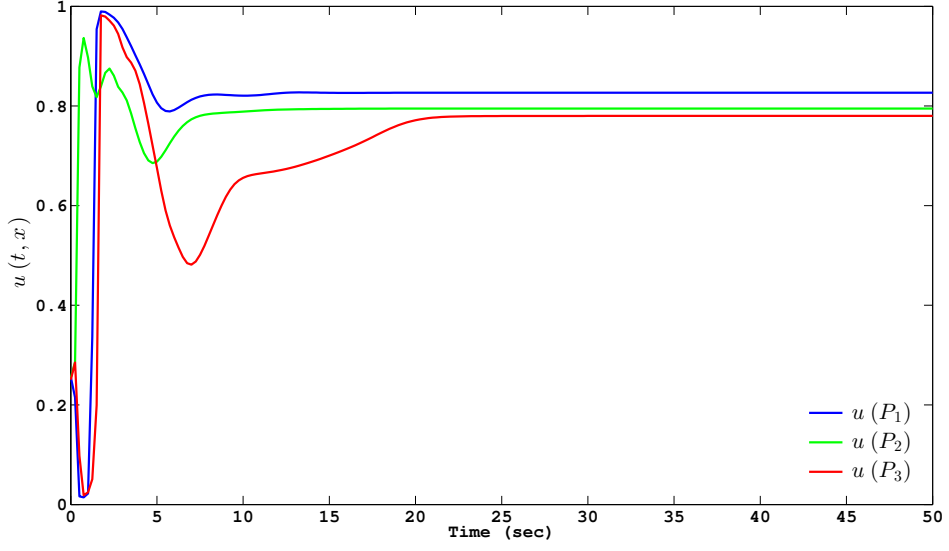


Figure 7: The evolution of the cell density with respect to the time at three different points: P_1 (5; 1.4) in the blue line, P_2 (6.25; 5.45) in the green line, P_3 (9.9; 8.05) in the red line.

assume that the diffusion tensors are anisotropic and heterogeneous, and are given by:

$$\Lambda(x) = D(x) = \begin{pmatrix} 1 & 0 \\ 0 & \lambda(x) \end{pmatrix}, \text{ with } \begin{cases} \lambda(x) = 0.5, & \text{if } x \in \Omega_1, \\ \lambda(x) = 1.5, & \text{if } x \in \Omega_2. \end{cases}$$

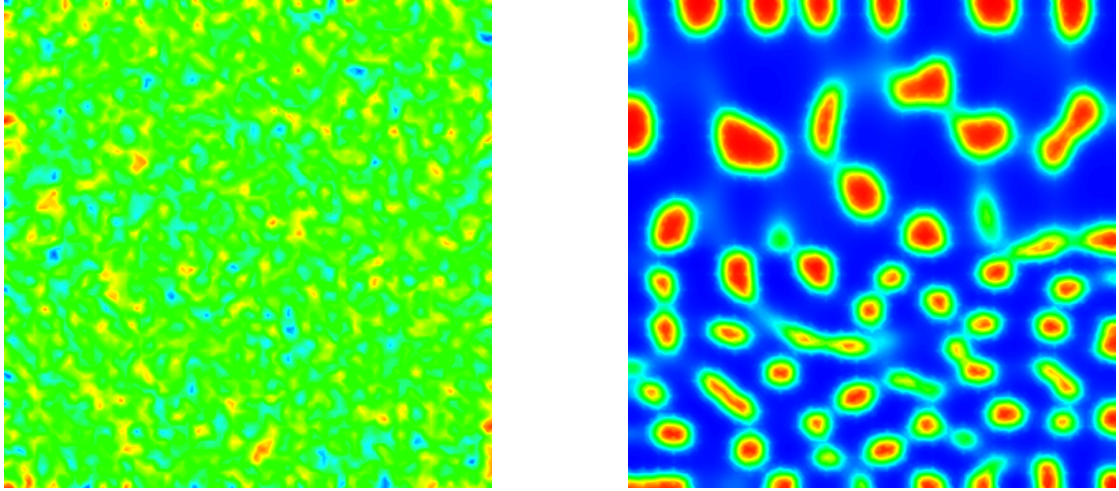


Figure 8: Pattern formation for the full chemotaxis model (2.1) on a 2-D domain $\Omega = (0, 10) \times (0, 10)$ at time $t = 0$ s with $0 \leq u \leq 1$ (left) and at time $t = 0.5$ s with $6.93 \times 10^{-3} \leq u \leq 0.99$ (right).

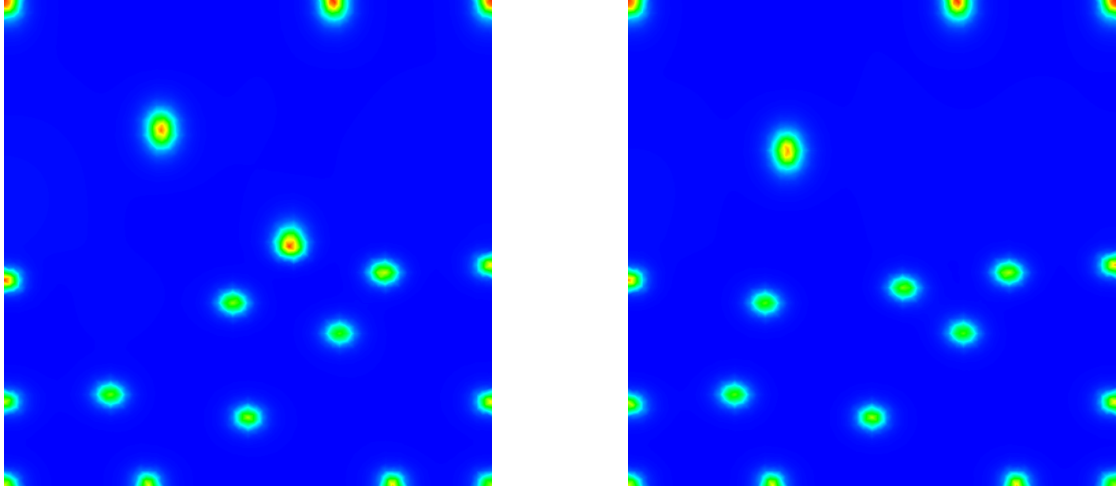


Figure 9: Pattern formation for the full chemotaxis model (2.1) at time $t = 49$ s with $3.67 \times 10^{-3} \leq u \leq 0.88$ (left) and at time $t = 150$ s with $4.3 \times 10^{-3} \leq u \leq 0.8447$ (right).

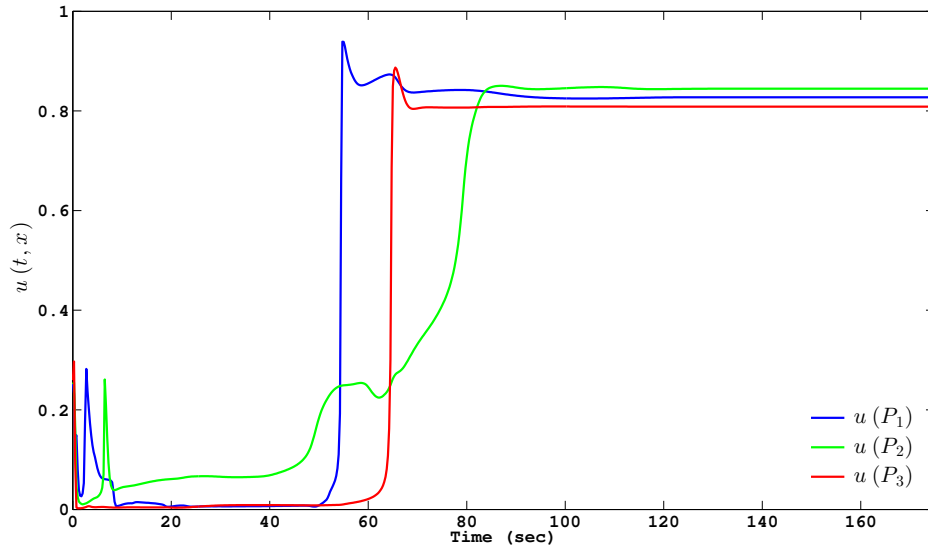


Figure 10: The evolution of the cell density with time at three different points: P_1 (5.70; 4.05) in the blue line, P_2 (3.28; 6.88) in the green line, P_3 (2.80; 3.75) in the red line.

Figures 8–9 show the evolution of spatial patterns for model (2.1) for different time moments. In region Ω_2 , where diffusion is more interesting in the y -axis direction, and at $t = 0.5$ s, we see that the aggregations form quickly, and they are much larger than those formed in region Ω_1 , which means that high diffusion in region Ω_2 (compared to that in region Ω_1) accelerate the merging process. On the other hand, at $t = 49$ s the aggregations in region Ω_2 disappear to form 5 spatial patterns; whereas, a plenitude of spatial patterns is seen in region Ω_1 compared

to region Ω_2 . Therefore, there exists a high dependence between the rate of diffusion and the generation of spatial patterns.

The time evolution for the last plot of figure 9 for different spots is given in figure 10. It shows that stationary spot patterns are obtained when $t \geq 125$ s.

Comparing figures 5-9, one can deduce that the patterning depends on diffusion coefficients, it is also known to depend on the size of the domain. These results prove the robustness of the *control volume finite element scheme* to capture spatial patterns for a volume-filling chemotaxis model with anisotropic diffusion tensors.

References

1. Tyson, R., Lubkin, S., Murray, J.. A minimal mechanism for bacterial pattern formation. *Proceedings of the Royal Society of London Series B: Biological Sciences* 1999;266(1416):299–304.
2. Murray, J.D.. How the leopard gets its spots. *Scientific American* 1988;258(3):80–87.
3. Turing, A.M.. The chemical basis of morphogenesis. *Bulletin of mathematical biology* 1990;52(1):153–197.
4. Murray, J., Myerscough, M.. Pigmentation pattern formation on snakes. *Journal of theoretical biology* 1991;149(3):339–360.
5. Painter, K., Maini, P., Othmer, H.. Stripe formation in juvenile pomacanthus explained by a generalized turing mechanism with chemotaxis. *Proceedings of the National Academy of Sciences* 1999;96(10):5549–5554.
6. Bendahmane, M., Saad, M.. Mathematical analysis and pattern formation for a partial immune system modeling the spread of an epidemic disease. *Acta applicandae mathematicae* 2011;115(1):17–42.
7. Chaplain, M.A., Ganesh, M., Graham, I.G.. Spatio-temporal pattern formation on spherical surfaces: numerical simulation and application to solid tumour growth. *Journal of mathematical biology* 2001;42(5):387–423.
8. Byrne, H., Chaplain, M.. Mathematical models for tumour angiogenesis: numerical simulations and nonlinear wave solutions. *Bulletin of Mathematical Biology* 1995;57(3):461–486.
9. Patlak, C.S.. Random walk with persistence and external bias. *The Bulletin of mathematical biophysics* 1953;15(3):311–338.
10. Keller, E.F., Segel, L.A.. Initiation of slime mold aggregation viewed as an instability. *Journal of Theoretical Biology* 1970;26(3):399–415.
11. Keller, E.F., Segel, L.A.. Model for chemotaxis. *Journal of Theoretical Biology* 1971;30(2):225–234.
12. Horstmann, D.. From 1970 until present: The keller-segel model in chemotaxis and its consequences ii. *Jahresbericht der Deutschen Mathematiker Vereinigung* 2004;106(2):51–70.
13. Andreianov, B., Bendahmane, M., Saad, M.. Finite volume methods for degenerate chemotaxis model. *Journal of computational and applied mathematics* 2011;235(14):4015–4031.

14. Eymard, R., Gallouët, T., Herbin, R.. Finite volume methods. *Handbook of numerical analysis* 2000;7:713–1018.
15. Eymard, R., Gallouët, T., Herbin, R.. Discretization of heterogeneous and anisotropic diffusion problems on general nonconforming meshes sushi: a scheme using stabilization and hybrid interfaces. *IMA Journal of Numerical Analysis* 2010;30(4):1009–1043.
16. Eymard, R., Gallouët, T., Herbin, R.. A finite volume scheme for anisotropic diffusion problems. *Comptes Rendus Mathématique* 2004;339(4):299–302.
17. Droniou, J., Eymard, R., Gallouët, T., Herbin, R.. Gradient schemes: a generic framework for the discretisation of linear, nonlinear and nonlocal elliptic and parabolic equations. *Mathematical Models and Methods in Applied Sciences* 2013;23(13):2395–2432.
18. Coudière, Y., Vila, J.P., Villedieu, P.. Convergence rate of a finite volume scheme for a two dimensional convection-diffusion problem. *ESAIM: Mathematical Modelling and Numerical Analysis* 1999;33(03):493–516.
19. Agouzal, A., Baranger, J., Maitre, J.F., Oudin, F.. Connection between finite volume and mixed finite element methods for a diffusion problem with nonconstant coefficients. application to a convection diffusion problem. *EAST WEST J NUMER MATH* 1995;3(4):237–254.
20. Cai, Z.. On the finite volume element method. *Numerische Mathematik* 1990;58(1):713–735. URL: <http://dx.doi.org/10.1007/BF01385651>.
21. Chavent, G., Jaffré, J., Roberts, J.. Mixed-hybrid finite elements and cell-centred finite volumes for two-phase flow in porous media. *Mathematical Modelling of Flow Through Porous Media* 1995;:100–114.
22. Eymard, R., Gallouët, T.. Convergence d'un schéma de type éléments finis-volumes finis pour un système formé d'une équation elliptique et d'une équation hyperbolique. *Modélisation mathématique et analyse numérique* 1993;27(7):843–861.
23. Affif, M., Amaziane, B.. Convergence of finite volume schemes for a degenerate convection–diffusion equation arising in flow in porous media. *Computer methods in applied mechanics and engineering* 2002;191(46):5265–5286.
24. Cariaga, E., Concha, F., Pop, I.S., Sepúlveda, M.. Convergence analysis of a vertex-centered finite volume scheme for a copper heap leaching model. *Mathematical Methods in the Applied Sciences* 2010;33(9):1059–1077.
25. Ohlberger, M.. A posteriori error estimates for vertex centered finite volume approximations of convection-diffusion-reaction equations. *ESAIM: Mathematical Modelling and Numerical Analysis* 2001;35(02):355–387.
26. Forsyth, P.A.. A control volume finite element approach to npl groundwater contamination. *SIAM Journal on Scientific and Statistical Computing* 1991;12(5):1029–1057.
27. Herbin, R., Hubert, F.. Benchmark on discretization schemes for anisotropic diffusion problems on general grids. *Finite volumes for complex applications V* 2008;:659–692.
28. Brauer, F., Castillo-Chavez, C.. Mathematical models in population biology and epidemiology. Springer; 2011.

29. Painter, K.J., Hillen, T.. Volume-filling and quorum-sensing in models for chemosensitive movement. *Can Appl Math Quart* 2002;10(4):501–543.
30. Stevens, A., Othmer, H.G.. Aggregation, blowup, and collapse: The abc’s of taxis in reinforced random walks. *SIAM Journal on Applied Mathematics* 1997;57(4):1044–1081.
31. Wang, Z., Hillen, T.. Classical solutions and pattern formation for a volume filling chemotaxis model. *Chaos: An Interdisciplinary Journal of Nonlinear Science* 2007;17(3):037108–037108.
32. Temam, R.. Navier-stokes equations. theory and numerical analysis. reprint of the 1984 edition. *AMS Chelsea, Providence, RI* 2001;.
33. Ibrahim, M., Saad, M.. Pattern formation and cross-diffusion for a chemotaxis model. In: *Conference Book Biomath 2013*. 2013;.